Utsunomiya *et al.*
Progress in Earth and Planetary Science (2023) 10:25
https://doi.org/10.1186/s40645-023-00558-y

Progress in Earth and Planetary Science

RESEARCH ARTICLE

Open Access

Basin-wide erosion and segmentation of the Plio-Pleistocene forearc basin in central Japan revealed by tephro- and biostratigraphy

Masayuki Utsunomiya[1*], Itoko Tamura[2], Atsushi Nozaki[3] and Terumasa Nakajima[4]

Abstract

The basement of the Tokyo metropolitan area consists of the Miocene–Pleistocene forearc basin fills that are well exposed around Tokyo Bay, especially on the Miura and Boso peninsulas. The forearc basin fills on these two peninsulas are called the Miura and Kazusa groups, and they were deposited during the late Miocene–Pliocene and Pliocene–middle Pleistocene, respectively. Because many biostratigraphic datum planes, paleomagnetic reversal events, and other chronostratigraphic tools are available for these deposits, they provide the "type stratigraphy" of other equivalent sedimentary sequences on the Japanese islands and in the northwest Pacific. However, the use of such stratigraphic markers has not been fully applied to understand the architecture of a basin-wide unconformity between the Miura and Kazusa groups called the Kurotaki unconformity. For our study, we made correlations among the Pliocene vitric tephra beds based on their stratigraphic levels, lithologic characteristics, the chemical compositions of glass shards, and calcareous nannofossil biostratigraphy. As a result, we were able to correlate tephra beds Ng-Ky25 just above the C3n.3n normal subchronozone (4.7 Ma), IkT16-An157.5 and IkT19-An158.5 near the top of the Mammoth reverse polarity subchronozone (3.21 Ma), and Ahn-Onr (2.6–2.7 Ma) across Tokyo Bay on the Miura and Boso peninsulas. We were able to recognize erosional surfaces and coeval mass-transport deposits immediately below the top of the Mammoth reverse polarity subchronozone, which suggests that submarine landslide(s) may have produced the lack of stratigraphic horizons (4.5–3.2 Ma) in the Miura and eastern Boso regions. Basal pebbly sandstone beds pervasively cover the erosional surfaces, and they show lateral variations into the thick (up to 60 m) mass-transport deposits and overlying turbidite sandstones. The lateral variations in sediment thickness of the post-failure deposits suggest that the basin-wide erosion was associated with the initial growth of a basin-bounding structural high that separates two distinct sub-basins in the forearc basin, which resulted in the subsequent onlapping deposition in the earliest stage of the Kazusa forearc basin. The basin-wide erosion marks the initiation of tectonic reconfigurations that led to segmentation of the forearc basin around the Tokyo Bay region.

Keywords Forearc basin fill, Kazusa group, Kurotaki unconformity, mass-transport deposit, Miura group, Pliocene, submarine landslide, tephra bed, Calcareous nannofossil

*Correspondence:
Masayuki Utsunomiya
m.utsunomiya@aist.go.jp
Full list of author information is available at the end of the article

1 Introduction

Forearc basins develop between volcanic arcs and trenches, and they are one of the basic components of a subduction system (Dickinson 1995). Their uplift and subsidence generally reflect long-term (at least 10–100 ky) depositional and tectonic processes due to forearc accretion and erosion (Clift and Vannucchi 2004; Takano et al. 2013; Noda 2016). It is known that forearc basin segmentation occurs because of the growth of zones of uplift and subsidence along the forearc wedge when subduction of the upper surface of a slab with a convex topography (e.g., seamounts; Tréhu et al. 2012) and/or oblique subduction take place (Wells et al. 2003; Okamura and Shishikura 2020). These processes affect the underlying accretionary wedge structure, which is closely related to the partitioning of the rupture zones of megathrust earthquakes (Sugiyama 1992; Wells et al. 2003; Fuller et al. 2006). Such segmentation is expected to be recorded as stratigraphic discontinuities and structural differences, and this might be recognized in ancient forearc basin fills that are exposed on land. However, very few cases of such stratigraphic discontinuities have been recognized, probably because the temporal accuracy is often not high enough to track major stratigraphic discontinuities across an entire basin in outcrops.

Forearc basins such as the Kumano Basin were developed along the Pacific side of the Japanese island arc, and their development has been affected by interactions of subduction tectonics and sedimentation (Underwood and Moore 2012). Using seismic facies and borehole data, the long-term evolution of these forearc basins has been discussed in terms of depositional processes (e.g., development of submarine fans) and the tectonic uplift/subsidence that produces unconformities (Takano et al. 2013; Moore et al. 2015; Kimura et al. 2018). In terms of forearc basin development owing to subduction of the Philippine Sea Plate, the Miocene–Pleistocene forearc basin fills that make up the basement of the Tokyo metropolitan area provide a good on-land analog of a modern forearc basin. The forearc basin fills are well exposed around Tokyo Bay, especially on the Miura and Boso peninsulas (Fig. 1). The deposits provide the type stratigraphy for other equivalent sedimentary sequences on the Japanese islands and in the northwest Pacific (Kazaoka et al. 2015; Ito et al. 2016), largely because they contain many marker tephra beds and well-preserved planktic microfossils that allow bed-by-bed correlations and estimates of sedimentary age.

There is a well-known stratigraphic discontinuity called the Kurotaki unconformity (Koike 1951) that divides the basin fill into the Miura (Awa) and Kazusa groups. The Kurotaki unconformity has received considerable attention because it was thought to represent a tectonic transition owing to a change in the direction of movement of the Philippine Sea Plate (Takahashi 2006), and also because other unconformities of similar age can be observed in the Japanese islands (Tamura and Yamazaki 2010; Oda et al. 2011). Meanwhile, the

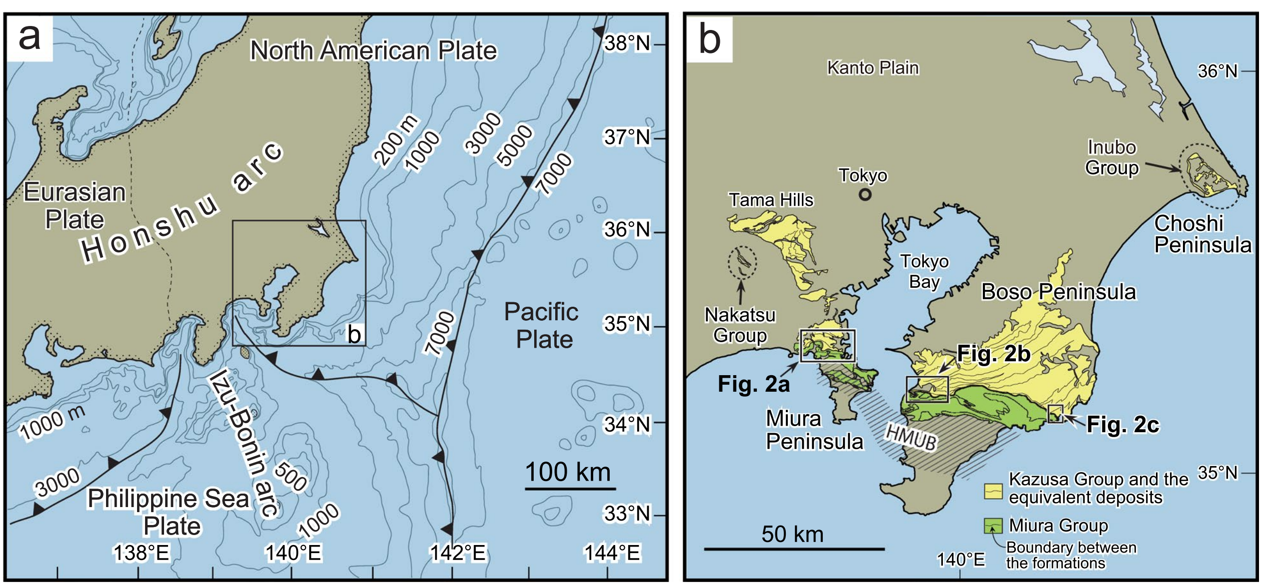

Fig. 1 Maps illustrating the geotectonic setting of the Miura and Kazusa groups in the southern Kanto region on the Pacific side of central Japan. **a** Present-day tectonic setting of central Japan. **b** Surface distributions of the Miura and Kazusa groups on the Miura and Boso peninsulas, based on Suzuki et al. (1995). Thinner lines within the yellow and green areas represent boundaries between formations. HMUB = Hayama – Mineoka uplift belt

chronostratigraphy of the Miura Peninsula, as reported by Utsunomiya et al. (2017), showed that continuous sedimentation occurred in the western part of the basin at the same time when the Kurotaki unconformity was forming in the eastern part, and this indicated the need for a better stratigraphic model to explain these regional differences. The purpose of our study was to construct a new stratigraphic model based on tephra bed correlations and calcareous nannofossil biostratigraphy. We revealed a previously overlooked major erosional surface and coeval mass-transport deposits (MTDs) in the forearc basin fills, and we discussed their significance for forearc basin segmentation.

2 Geologic setting

2.1 Forearc basin fills: the Miura and Kazusa groups

The central part of the Honshu arc is located near a trench–trench–trench-type triple junction (Fig. 1a) where the Philippine Sea Plate is subducting beneath the North American Plate and the Pacific Plate is subducting beneath the North American and Philippine Sea plates (McKenzie and Morgan 1969). Deformation of the Neogene deposits exposed on the Miura and Boso peninsulas records compressional convergence owing to the interaction of the Philippine Sea and Eurasian plates near the triple junction after the Miocene (Ogawa et al. 1989). In this tectonic setting, the Hayama–Mineoka uplift belt consists of an ophiolitic complex that acted as a trench–slope break (Takahashi 2008) that created space for the deposition of the forearc basin fill (Fig. 1b). The forearc basin fills on the Miura and Boso peninsulas are called the Miura (middle Miocene–Pliocene) and Kazusa (Pliocene–middle Pleistocene) groups, which are approximately 2000 and 3000 m thick, respectively (Suzuki et al. 1995). These groups consist of shallow- and deep-marine deposits (Mitsunashi and Kikuchi 1982; Ito and Katsura 1992), and they contain numerous marker tephra beds and abundant microfossils that facilitate lateral stratigraphic correlations and reliable determinations of depositional age (e.g., Sato and Takayama 1988; Pickering et al. 1999). Moreover, the fact that the tephra beds act as stratigraphic markers and can be traced laterally has allowed sedimentologists to recognize spatial variations in the depositional sequences (Ito 1992a, b, 1995), the sandstone beds in submarine fans (Hirayama and Nakajima 1977), and large-scale mass-transport deposits (Utsunomiya 2018; Utsunomiya et al. 2018; Utsunomiya and Yamamoto 2019). Previous studies on stratigraphic correlations between the Boso and Miura peninsulas (Ida et al. 1956; Mitsunashi 1973; Mitsunashi and Kikuchi 1982; Suzuki et al. 1995) have been based mainly on similarities of the macroscopic and microscopic characteristics of the marker tephra beds. A combination of microfossil biostratigraphy and the geochemical compositions of volcanic glass in the tephra beds allowed significant improvements in correlating the stratigraphic units of Pleistocene sequences around Tokyo Bay, such as on the Miura, Boso, and Choshi peninsulas (marine deposits) and in the Tama hills (terrestrial and shallow marine deposits) (Fujioka et al. 2003; Fujioka and Kameo 2004; Takahashi et al. 2005; Tamura et al. 2010, 2019; Mizuno and Naya 2011; Suzuki and Murata 2011; Utsunomiya et al. 2019). The stratigraphy established for the Miura and Boso peninsulas has played a significant role in interpretations of seismic profiles (Chiba Prefecture 2004; Asao and Ito 2011) and deep-borehole sequences around Tokyo Bay (Suzuki and Horiuchi 2002; Yanagisawa et al. 2006; Chiyonobu et al. 2007; Naya et al. 2013). Moreover, the tephra beds of the Kazusa Group recently recognized at depth (> 1000 m) around Tokyo Bay (Tamura et al. 2010; Utsunomiya et al. 2020) have allowed the integration of seismic-scale structures with the high-resolution stratigraphy established from outcrop-based studies.

The boundary between the Kazusa and Miura groups is called the Kurotaki unconformity, with the lower Kazusa Group lapping onto the underlying Miura Group as the depocenter of the Kazusa Group migrated northward (Mitsunashi and Yamauchi 1988). On the Boso Peninsula, the unconformity between the Kazusa and Miura groups is distinctly angular, representing a temporal gap from ca. 3 to 2.4 Ma (Kameo and Sekine 2013), but on the Miura Peninsula there is no significant angular relationship between the two groups (Koike 1951; Akamine et al. 1956). No significant temporal gap corresponding to the Kurotaki unconformity has been identified in the Inubo Group, exposed on the Choshi Peninsula, based on biostratigraphy and tephrostratigraphy (Sakai 1990; Tamura and Yamazaki 2010; Tamura et al. 2014). Utsunomiya et al. (2017) demonstrated that the uppermost parts of the Miura Group and the lowermost parts of the Kazusa Group on the Miura Peninsula are time-equivalent deposits, based on the lateral tracing of tephra beds. Gradual variations in the rate of sedimentation indicated that the Kazusa Group of the Miura Peninsula was deposited conformably on the Miura Group during 3.2–2.4 Ma, based on calcareous nannofossil biostratigraphy and magnetostratigraphy. The stratigraphic flamework is therefore being reconstructed with a focus on Pliocene stratigraphy as the key interval.

2.2 Miura peninsula

The geologic map of the northern Miura Peninsula in Fig. 2a has been modified from Eto (1986a), Eto et al. (1998) and Utsunomiya et al. (2017) based on the distribution of tephra beds shown by Inagaki et al. (2007), Utsunomiya et al. (2017), and this paper. The Miura and

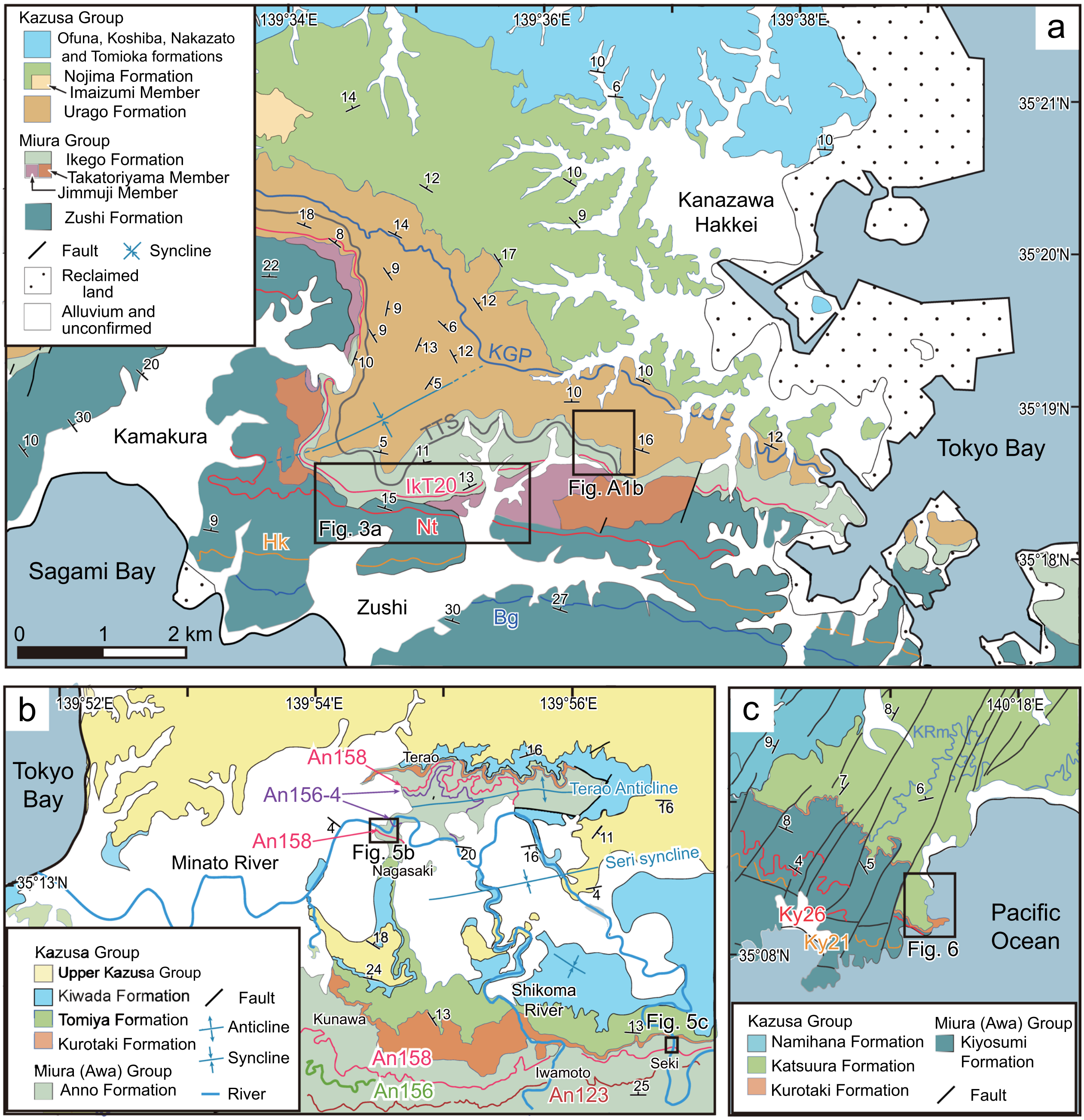

Fig. 2 Geologic maps of **a** the northern Miura Peninsula (Eto 1986a; Eto et al. 1998; Utsunomiya et al. 2017), **b** the western Boso Peninsula (Nakajima and Watanabe 2005), and **c** the central Boso Peninsula (Tokuhashi and Ishihara 2008)

Kazusa groups generally dip 5–30°NE, but the Miura Group and the lowermost parts of the Kazusa Group have been deformed by a NE–SW trending syncline. The Miura Group consists of the Miocene–Pliocene Zushi and the Pliocene Ikego formations, in ascending stratigraphic order. A basal conglomerate called the Tagoegawa sandstone and conglomerate Member (15–50 m in thickness) is overlain by mudstone-dominated alternating sandstones and mudstones (1000–1500 m in thickness) of the Zushi Formation (Eto et al. 1998). The lower part of the Ikego Formation consists of the Takatoriyama volcaniclastic Member (0–210 m in thickness) and the Jimmuji volcaniclastic and mudstone Member (0–60 m in thickness), and the main upper part of the Ikego Formation consists of alternating beds of sandstone and tuffaceous sandy mudstone 150–400 m in thickness

(Eto et al. 1998). In detail, the Takatoriyama Member consists of massive and cross-bedded tuffaceous sandstones and conglomerates that have been interpreted as canyon-fill deposits, given the convex-down shape inferred from their geographic distribution (Soh et al. 1991). The Jimmuji Member consists of mass-transport deposits (Fig. 3b; Eto 1993; Yokohama Defense Facilities Administration Bureau 1993) that contain chaotic deposits with blocks of sandstone and mudstone, likely generated by submarine landslides of both the canyon wall and the canyon fill (Taira et al. 1993). The upper Ikego Formation consists mainly of alternating beds of sandstone and tuffaceous sandy mudstone, which cover an irregular erosional surface of a slide block of sandy mudstone in the Jimmuji Member (Fig. 3; Eto 1993; Yokohama Defense Facilities Administration Bureau 1993; Utsunomiya et al. 2017). The lowermost part of the Kazusa Group, the Urago Formation, consists mainly of tuffaceous medium- to coarse-grained sandstones and tuffaceous muddy sandstones (Utsunomiya and Majima 2012). Trough- and tabular-cross bedding is common in the tuffaceous sandstones, and this has been attributed to the migration of dunes under the influence of bottom currents that varied in direction between northward and eastward (Utsunomiya et al. 2015).

The paleobathymetry of the upper Ikego Formation and the Urago Formation has been estimated at between 500 and 2000 m based on benthic foraminiferal assemblages (Eto et al. 1987) and between 400 and 600 m based on molluscan asemblages (Utsunomiya and Majima 2012). The upper part of the Ikego Formation has been assigned to the CN12a subzone of Okada and Bukry (1980) by Okada (1993) and to the RN12 Zone of Kamikuri et al. (2009) by Suzuki and Kanie (2012).

Although the top of the Ikego Formation has been interpreted as the westward extension of the Kurotaki unconformity (Mitsunashi 1973; Eto 1986b; Eto et al. 1998), the bedding planes of the Ikego Formation are almost parallel to those of the overlying Kazusa Group (Koike 1951; Akamine et al. 1959). Utsunomiya et al. (2017) demonstrated that the Urago Formation of the Kazusa Group conformably overlies the Ikego Formation, based on tephra bed correlation, then identified the following stratigraphic markers in ascending order (Fig. 4): top (3.21 Ma) of the Mammoth subchronozone (C2An.2r); base (3.13 Ma) and top (3.05 Ma) of the Kaena subchronozone (C2An.1r); last appearance of *Discoaster tamalis* (MIS G7–G8, 2.76 Ma; Kameo and Okada 2016); the widespread tephra bed KGP (ca. 2.5 Ma); and the last appearance of *Discoaster pentaradiatus* (MIS 95, 2.41 Ma; Kameo and Okada 2016). The KGP tephra bed occurs within the lowermost Matuyama chronozone (Tamura et al. 2010; Ueki et al. 2013), which suggests the Gauss–Matuyama boundary (2.61 Ma) is in the middle of the Urago Formation.

2.3 Boso peninsula

The geologic maps of the western (Fig. 2b) and eastern (Fig. 2c) Boso Peninsula are from Nakajima and Watanabe (2005) and this study, respectively. Although the Miura Group on the Boso Peninsula is often called the Awa Group (Nakajima et al. 1981; Nakajima and Watanabe 2005), for convenience we use the name Miura Group following Suzuki et al. (1995) in order to identify time equivalent strata on both peninsulas. The Miura Group on the western Boso Peninsula generally strikes E–W, and it has been deformed by ENE–WSW trending folds (the Seri Syncline and Terao Anticline: Fig. 2b). On the central Boso Peninsula, the fold axes trend ESE–WNW, and the folds are called the Kiyosumi syncline and Kiyosumi anticline. The Miura Group on the Boso Peninsula consists of the Fukawa, Kanigawa, Kinone, Amatsu, Kiyosumi, and Anno formations in ascending stratigraphic order (Nakajima et al. 1981), among which the Kiyosumi and Anno formations were the subject of our study.

The Kiyosumi Formation consists mainly of alternating beds of hemipelagic mudstone and sandstone, and it varies in thickness from 76 to 196 m on the western side (Nakajima 2005) to ~ 800 m in the center of the peninsula (Tokuhashi and Ishihara 2008). The Kiyosumi Formation represents sand-dominated submarine fan deposits with a feeder system from north to south (Tokuhashi 1989). The spatial–temporal distribution of turbidite deposits shows the development of syn-sedimentary E–W trending folds, which resulted in the strata being thicker along the synclinal axis (Tokuhashi 1976a, b; Tokuhashi 1989). The paleobathymetry of the Kiyosumi Formation has

(See figure on next page.)

Fig. 3 Distribution and outcrop occurrences of the Zushi Formation, the Jimmuji Member, and the upper part of the Ikego Formation. **a** Geologic map of the Hisagi and Ikego areas, Zushi City, showing the locations of the sketched outcrops reported by previous researchers, and the locations of the studied sites. Gray-colored strike and dip symbols are from Eto (1993). **b** Sketches of outcrops exposed by residential construction illustrate stratigraphic levels of the Nt and Ng tephra beds and the internal structure of the Jimmuji Member (after Eto 1993, and Yokohama Defense Facilities Administration Bureau 1993). **c** Route maps in the Ikego Forest Natural Park showing location of outcrops of the Zushi and Ikego formations. **d** Geologic columns along traverses Z1 and Z2 where the uppermost part of the Zushi Formation and the overlying Ikego Formation are exposed. Note that the Jimmuji Member becomes thinner and pinches out westward where a tens of cm-thick pebbly sandstone bed covers the erosional surface. The lithologic legend is shown in Fig. 4

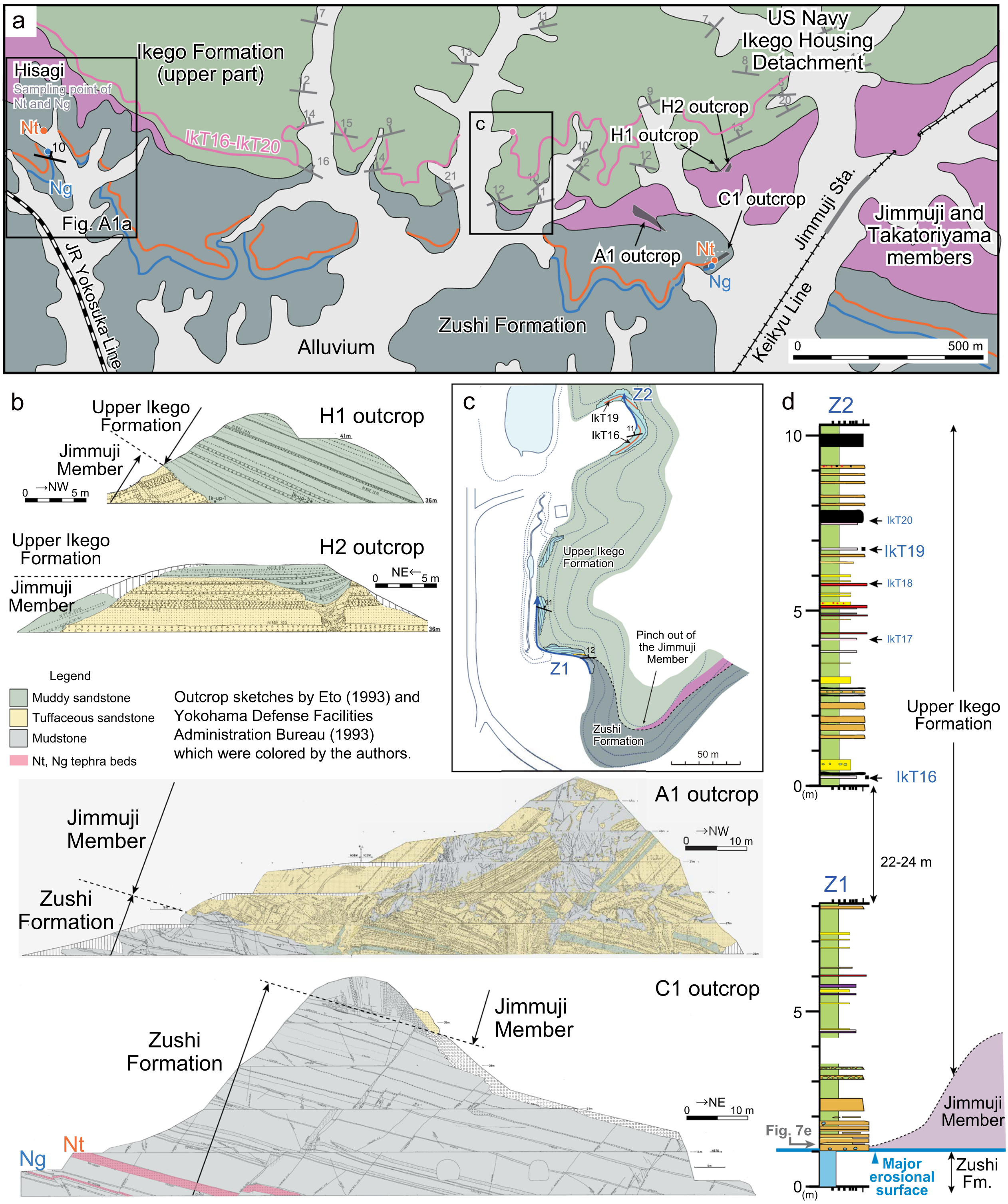

Fig. 3 (See legend on previous page.)

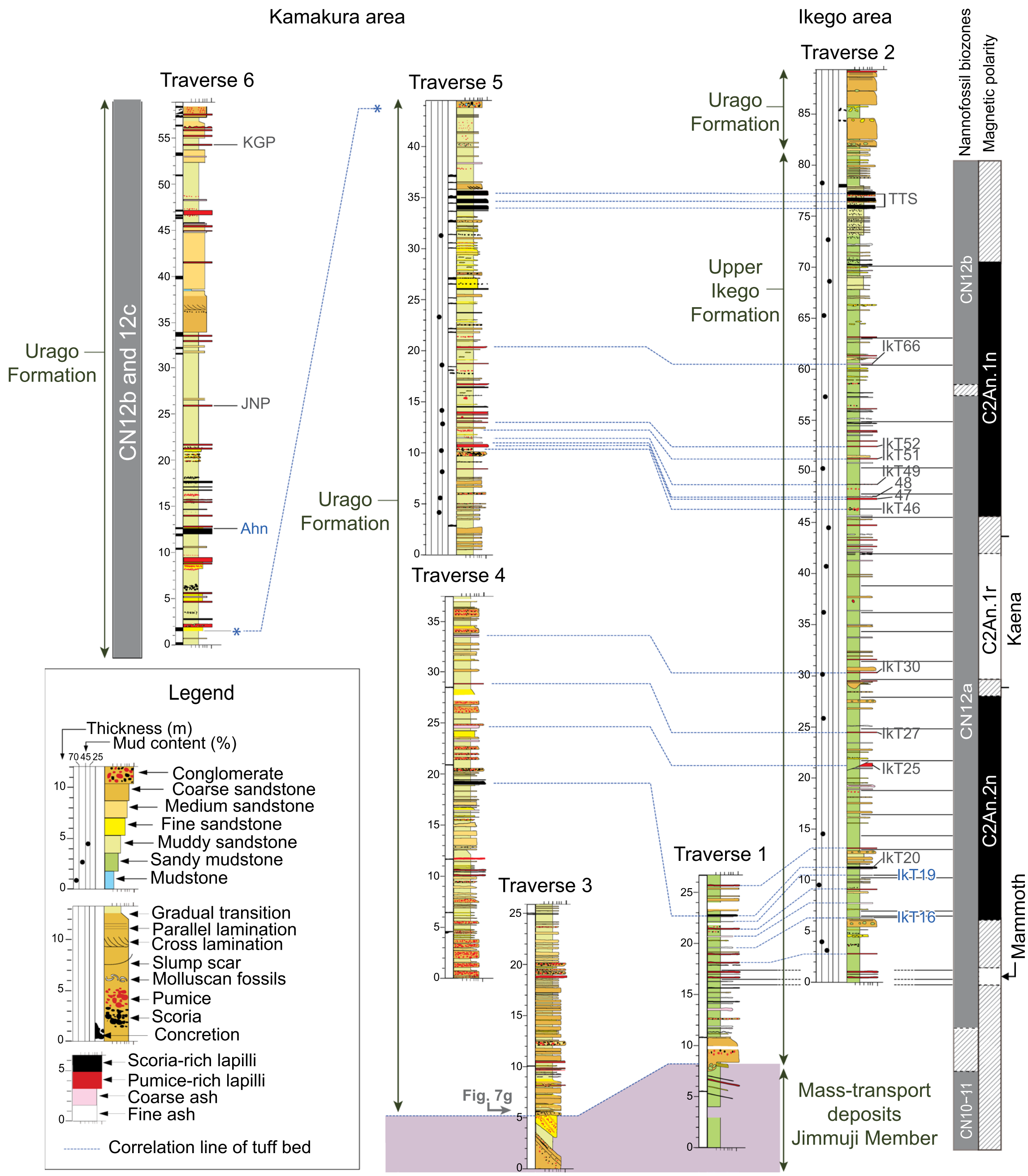

Fig. 4 Geologic columns of the Ikego and Urago formations, Miura Peninsula (after Utsunomiya et al. 2017), showing magnetic polarity and calcareous nannofossil biozones. Note that tephra beds IkT16 and 19 are intercalated immediately above the top of the Mammoth subchronozone. Ahn is within CN12b–c. Ahn is between the top of *Discoaster tamalis* (2.76 Ma) and tephra bed KGP (ca. 2.5 Ma), which is consistent with the estimated age of the widespread tephra UN-MD2 (2.7–2.6 Ma). The calcareous nannofossil zonal scheme follows that of Okada and Bukry (1980). The notation of the paleomagnetic polarity zones is from Ogg (2020)

been estimated to be 1000–1800 m (Hatta and Tokuhashi 1984), based on benthic foraminiferal assemblages.

The Anno Formation conformably overlies the Kiyosumi Formation and is unconformably overlain by the Kazusa Group across the Kurotaki unconformity. The thickness of the Anno Formation is 125–386 m in the western part of the Boso Peninsula (Nakajima 2005). Previous studies numbered the marker tephra beds in the Anno Formation in ascending stratigraphic order with numbers prefixed by "An" (Nakajima et al.

1981; Natural History Museum and Institute, Chiba, 1995, 1996; Nakajima 2005). In the western part of the peninsula, the Anno Formation generally shows an upward-coarsening succession from mudstone, sandy mudstone, and muddy sandstone to sandstone (Nakajima 2005). The Anno Formation represents submarine fan deposits (Nakajima et al. 1981; Ishihara and Tokuhashi 2005) or a slope base system (Saito and Ito 2002). Ishihara and Tokuhashi (2005) recorded the lateral distribution and successive changes in the turbidite facies and paleocurrent directions. They identified six sedimentary facies associations: channel fill deposits of pebbly sandstone and conglomerates; natural levee deposits of alternating thin turbidites and hemipelagic mudstones; thick-bedded lobe deposits; marginal deposits of alternating thin turbidites and hemipelagic mudstones; marginal deposits of alternating hemipelagic mudstones and tephra beds; and extensive slump deposits. The upper part of the Anno Formation consists of marginal deposits of alternating hemipelagic mudstones and tephra beds that coarsen upward, suggesting a shallower depositional environment or the winnowing of fine-grained sediment owing to bottom currents (Ishihara and Tokuhashi 2005). There are many mass-transport deposits in the Anno Formation, of which “Ta slump” below An22 and “Sak slump” below An157 can be traced laterally (Nakajima 2005). There is a hiatus due to submarine landslide(s) and residual mass-transport deposits called “Sak slump” between An155 and An157 (Fig. 5). Sak slump ranges in thickness from 0.2 to 5 m, and it caused the erosion of 8–15 m-thickness of underlying strata, including tephra beds An155-2–An156-4 (Nakajima 2005). The paleobathymetry of the Anno Formation has been estimated to be 1200–2800 m (Hatta and Tokuhashi 1984), based on benthic foraminiferal assemblages.

The depositional ages of the Kiyosumi and Anno formations have been estimated using calcareous nannofossil biostratigraphy (Kameo et al. 2010; Kameo and Sekine 2013), fission-track analyses of the tephra beds (Kasuya 1987; Tokuhashi et al. 2000), and magnetostratigraphy (Niitsuma 1976; Haneda and Okada 2019, 2022). The Kiyosumi Formation includes C3n.4n and C3n.3n normal polarity subchronozones, and the top of this formation belongs to the C3n.2n normal polarity subchronozone (Niitsuma 1976; Takahashi 2008). Haneda and Okada (2019) recognized the period in the Anno Formation that extends from the top of the Nunivak normal polarity subchronozone (4.49 Ma) to the top of the Mammoth reverse polarity subchronozone (3.21 Ma). The Sak slump is intercalated within the Mammoth subchronozone, and it may have caused the erosion of strata over a period of approximately 90 kyr (Haneda and Okada 2019).

The Kazusa Group on the Boso Peninsula is made up of a shallow- to deep-marine succession that is ~ 3 km thick (e.g., Ito and Katsura 1992; Suzuki et al. 1995) in the middle of the peninsula (Nakajima and Watanabe 2005; Utsunomiya and Ooi 2019). The Kazusa Group is divided into 13 formations based on lithofacies and stratigraphic positions. The lower and middle parts of the Kazusa Group consist of deep-sea (submarine fan and basin plain), upper slope, and outer shelf deposits, whereas the upper parts of the Kazusa Group comprise shallow marine deposits (Ito and Katsura 1992). The Kazusa Group laps onto the Miura Group, and this resulted in the base of the Kazusa Group younging toward the central part of the peninsula. The basal sandstone and conglomerate succession called the Kurotaki Formation is thought to be contemporaneous with the laterally adjacent turbidite successions of the lower part of the Kazusa Group on the eastern and western sides of the peninsula (Kawabe et al. 1981; Ito et al. 1992; Nakajima and Watanabe 2005). The paleoslope dips southeastward in the lower part of the Kazusa Group and northeastward in the middle and upper parts, as inferred from paleocurrent analyses of the turbidites (Hirayama and Nakajima 1977; Tokuhashi 1992).

2.4 Widespread tephra beds used for inter- and intra-basinal correlation

There are many widespread vitric ash beds intercalated in the Miura Group and the lower parts of the Kazusa Group on the Boso Peninsula, and these tephra beds are also distributed around the Tokai, Kinki, and Chubu districts in the western Japanese islands. In the Miura Group, tephra beds An51, An53, An77, An85, An112, An129, and An130 are regarded as widespread tephra beds named Trb1-Ya4, Sk-Ya5, Ksg-An77, Znp-Ohta, Ymp-SF8.3, Hgs-An129, and Sr-Ity, respectively (Kurokawa and Higuchi 2004; Satoguchi et al. 2005; Tamura et al. 2008; Tamura and Yamazaki 2010; Satoguchi and Nagahashi 2012). In the lower parts of the Kazusa Group, KW2, KH1, MY, KB, HS C, Kd44, Kd39, Kd25, and Kd24 are regarded as widespread tephra beds named Fup-KW2, Obr-Bnd1, OM1-OKIII, Bnd2-O1, Tmg-R4, Kd44-Nk, Ho-Kd39, Eb-Fukuda, Om-SK110, and Srt-SK100, respectively (Nagahashi et al. 2000; Suzuki and Nakayama 2007; Tamura et al. 2019). Moreover, some thick (several meters) crystal-rich tephra beds with a “salt and pepper” appearance have been used for intra-basinal correlation. For example, Am78, Ky21, and Ky26 on the Boso Peninsula have been correlated with Ok, Hk, and Nt on the Miura Peninsula (Urabe et al. 1990; Urabe 1992; Suzuki et al. 1995).

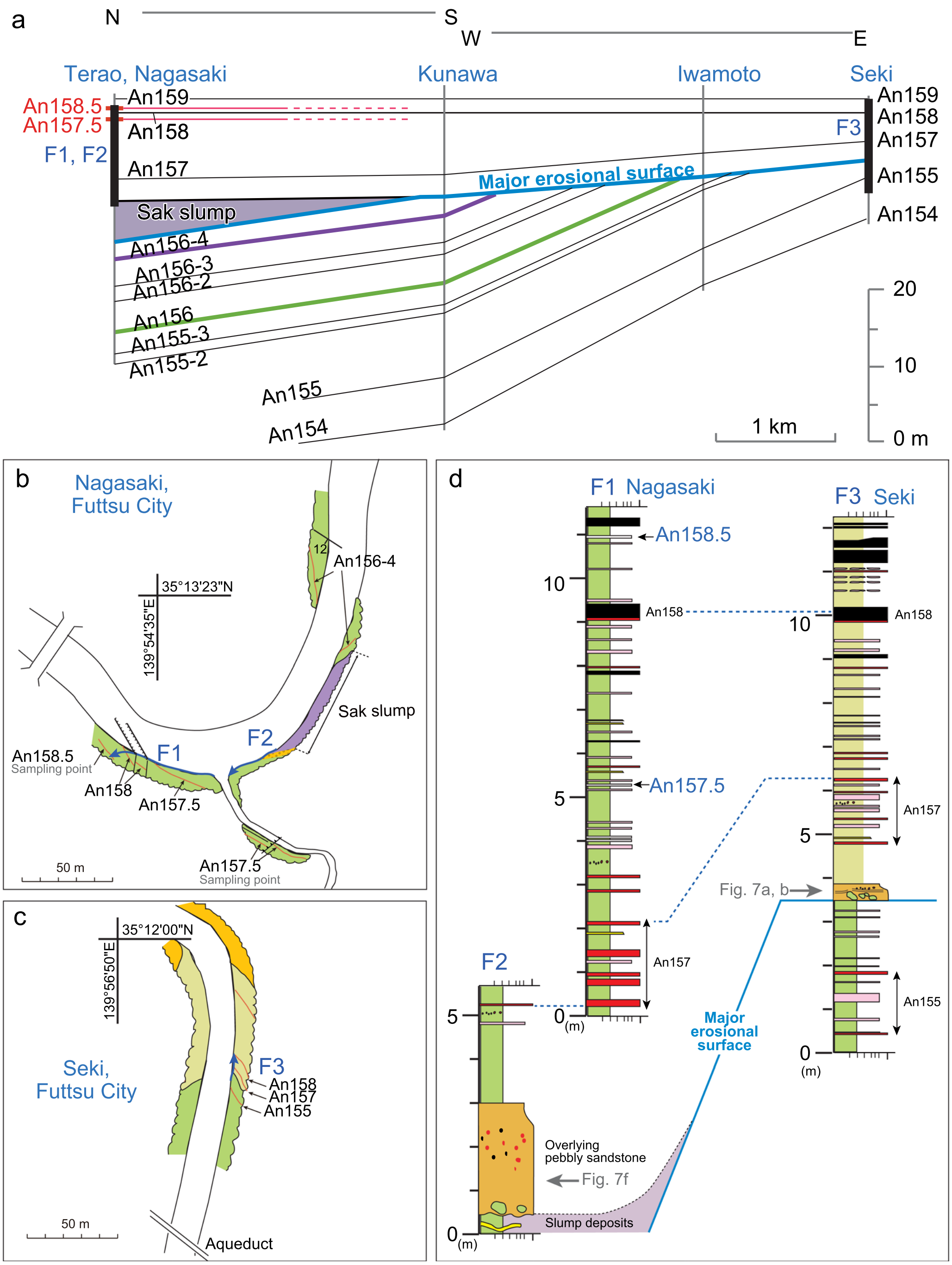

Fig. 5 Geologic cross section, route map, and geologic columns of the Anno Formation on the western Boso Peninsula. **a** Stratigraphic correlation of the uppermost part of the Anno Formation showing east–west (Kobata–Iwamoto–Kunawa) and south–north (Kunawa–Terao, Nagasaki) variations in horizons underlying the Sak slump and the equivalent erosional surface (blue line). **b**, **c** Route maps in Nagasaki **b** and Seki **c** with outcrops of the upper part of the Anno Formation. **d** Geologic columns of part of the Anno Formation that shows lateral facies changes, based on tephra bed correlation. In a similar manner to the Ikego area (Fig. 3), a mass-transport deposit named "Sak slump" becomes thinner and pinches out eastward where a tens of cm-thick pebbly sandstone bed covers the erosional surface. The lithologic legend is shown in Fig. 4

3 Methods

We used visual observations to describe the lithologies and thicknesses of tephra beds, and we classified the tephra beds according to the dominant grain size as fine ash (< 63 µm), coarse ash (63 µm–2 mm), and lapilli (> 2 mm), following the classification scheme of Heiken and Wohletz (1985). Lapilli-dominated beds were classified into pumice-rich lapilli beds and scoria-rich lapilli beds, based on the dominant grain component. Tephra samples (10–50 cc) were washed using a disposable nylon mesh sieve to remove fine-grained particles (< 63 µm), and they were then cleaned using gentle ultrasonication to remove clay minerals. After that, the samples were dried at less than 60 °C for half a day in a constant-temperature drying oven. The very-fine sand-sized particles (63–125 µm) were collected using a disposable nylon mesh sieve with a pore size of 125 µm, and these particles were then fixed onto a glass slide using the optical adhesive Nd = 1.545, produced by Furusawa Geological Survey, Co. Ltd., and then cured under ultraviolet light. These slides were then used to examine the shapes of glass shards and to identify the dominant heavy minerals using a polarizing light microscope (BX-53, Olympus Co., Tokyo, Japan) with a magnification of 100× under both cross-polarized and plane-polarized light. The glass shard classification used follows Kishi and Miyawaki (1996). Refractive index measurements of glass shards were performed using the refractometer system MAIOT (Furusawa Geological Survey, Co. Ltd.), as described by Furusawa (1995). The major and trace element compositions of the glass shards (10–15 grains) were determined using EDX (energy dispersive X-ray spectrometry) and LA–ICP–MS (laser ablation inductively coupled plasma mass spectrometry), following Furusawa (2017). Major element compositions were determined using EDX (EMAX Evolution EX-270, HORIBA, Ltd.) by scanning 4×4 µm areas of the polished surfaces of glass shards with an electron beam (90 nm beam size) for 50 s under an SEM (scanning electron microscope SU1510, HITACHI High-Tech Corp). Trace element compositions were measured bringing particles generated from a laser ablation system (LSX-213 G2 + [Nd: YAG 213 nm], TELECYNE, Ltd.) into ICP–MS (iCAP Qc, Thermo Fisher Scientific, Inc.) using helium as the carrier gas. GSE-1G from the United States Geological Survey was used as a reference glass.

The sediment samples used for analyses of calcareous nannofossils were collected from fresh outcrop surfaces using a chisel or portable drill. Smear slide samples were prepared by fixing sediment samples onto a glass slide using the optical adhesive GL-4006 (Gluelabo Ltd., Mie, Japan) and then cured under ultraviolet light. These slides were then examined using a polarizing light microscope (BX-53, Olympus Co., Tokyo, Japan) with a magnification of 1500× under cross-polarized and plane-polarized light. We used the zonal schemes of Okada and Bukry (1980). The ages of the datum planes follow Raffi et al. (2006) and Raffi et al. (2020).

4 Results

4.1 Lithostratigraphy and sedimentary structures

In this section, we describe the local stratigraphic and sedimentary characteristics for deposits around the major erosional surface in the following three regions: the Miura Peninsula (Figs. 3, 4), the western Boso Peninsula (Fig. 5), and the eastern Boso Peninsula (Fig. 6).

4.1.1 Miura peninsula

The uppermost part of the Zushi Formation, the Jimmuji Member, and the upper part of the Ikego Formation are exposed in Zushi City (Fig. 3a). The Zushi Formation consists mainly of mudstones in which thin (< 20 cm) sheet-like sandstones and two vitric tephra beds Nt (Urabe 1998) and the newly named Nagoe (Ng) are intercalated. Ng is a synonym of the Nt-mid of Eto (1993). Ng is intercalated 8–9 m below Nt (Additional file 1: Fig. A1) at a location 100 m east of the outcrop described by Urabe (1998). Both these tephra beds can also be recognized in the C1 outcrop that was exposed during residential constructions (Fig. 3b). The two basal slide planes of the mass-transport deposits of the Jimmuji Member are located 37 and 38 m above the top of Nt (Fig. 3b; Eto et al. 1993; Yokohama Defense Facilities Administration Bureau 1993). Chaotic deposits and slide blocks of sandstone and mudstone in the Jimmuji Member are well exposed in the A1 outcrop (Fig. 3b). The Jimmuji Member becomes thinner and pinches out westward, where a tens of cm-thick pebbly sandstone bed covers the erosional surface (Figs. 3b, d, 7e). The upper part of the Ikego Formation (90 m thick) is exposed continuously along traverses 1 and 2 of Utsunomiya et al. (2017) (Figs. 4, Additional file 1: A1, A2) and along traverses Z1 and Z2 in the Ikego Forest Natural Park (Fig. 3c, d). Tephra beds were numbered in ascending stratigraphic order and prefixed with "IkT", and some of these were traced laterally by Utsunomiya et al. (2017) (Fig. 4). The stratigraphic levels of all IkT tephra beds are shown in Additional file 1: Fig. A2.

Here we provide details of the lithologies and chemical compositions of IkT16 and IkT19 in the Ikego Formation and Ahn in the Urago Formation. IkT19 was first reported by Tamura et al. (2014) as Ikego 1 (Ikg1), which was correlated with a tephra bed named In1 in the Inubo Group on the Choshi Peninsula, based on petrography and the chemical compositions of glass shards. Here, we

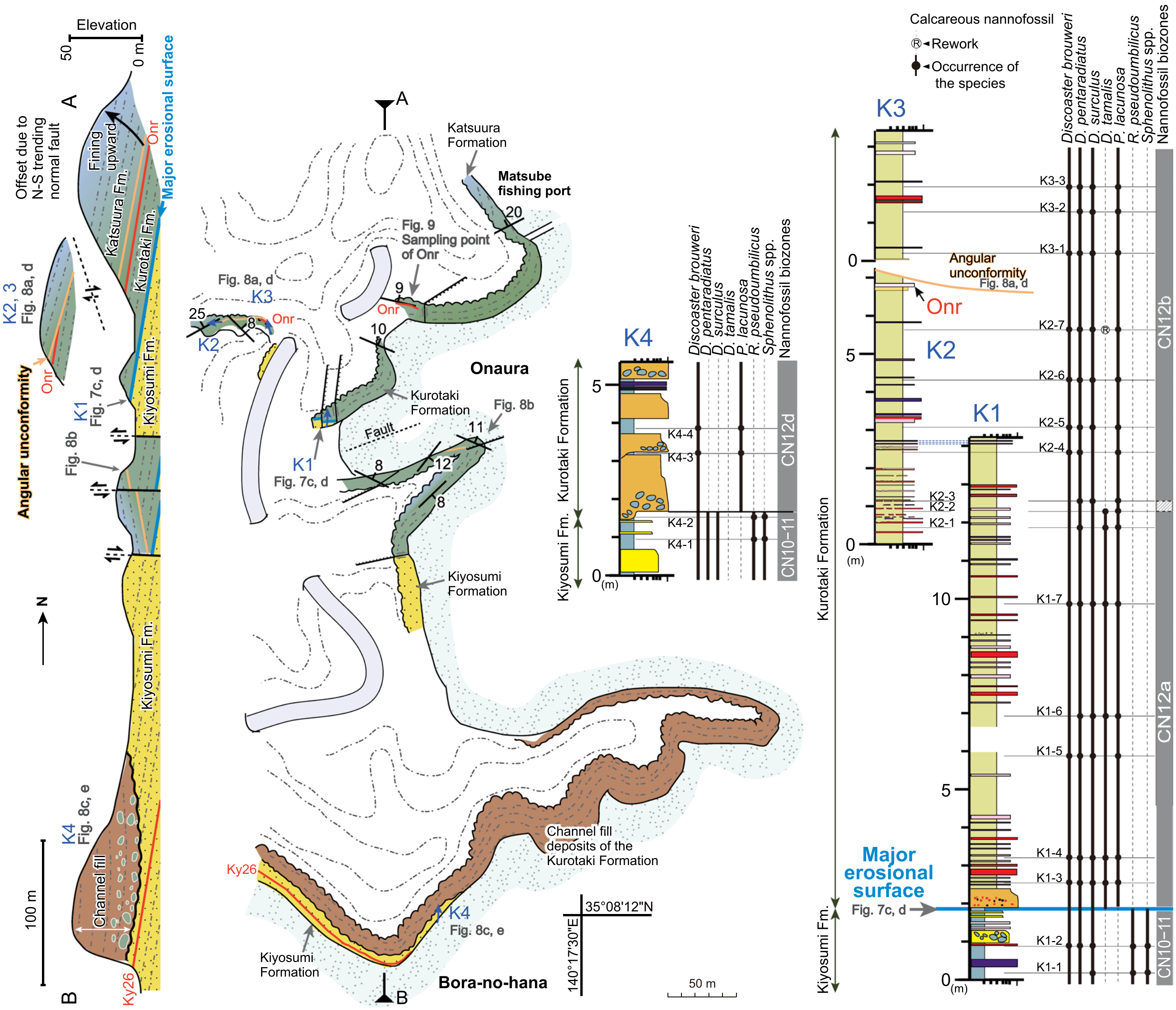

Fig. 6 From left to right, cross section, geologic map, geologic columns, and stratigraphic distribution of calcareous nannofossils in Onaura, Katsuura City, eastern Boso Peninsula. The lithologic legend is shown in Fig. 4

use the tephra name IkT19 instead of Ikg1 for consistency with the numbering used by Utsunomiya et al. (2017). Ahn in the Urago Formation was reported by Tamura and Yamazaki (2010), and this bed is the same as AhG named by Tamura et al. (2010). This tephra bed has been correlated with the widespread tephra UN-MD2 (2.6–2.7 Ma), based on petrography and the chemical compositions of glass shards (Tamura and Yamazaki 2010).

4.1.2 Western Boso peninsula

The uppermost part of the Anno Formation is well exposed along the Minato River and the branch streams in Futtsu City, on the western side of the Boso Peninsula (Figs. 2b, 5). Stratigraphic cross-sections (Fig. 5a) from east to west (Seki–Iwamoto–Kunawa) and from south to north (Kunawa–Terao, Nagasaki) show that the thickness between An154 and An157 varies laterally owing to erosion by submarine landslide(s) that resulted in a mass-transport deposit (MTD) (Figs. 5d, 7f). This MTD is named the "Sak slump" (Nakajima 2005), and the equivalent erosional surface cuts the underlying strata (blue line in Fig. 5a). At outcrop, the MTD pinches out eastward, and pebbly sandstones cover the erosional surface (Figs. 5d, 7a, b). Undulating parallel or low-angle cross stratification is weakly developed in these sandstones. We have not determined the paleocurrent directions of the pebbly sandstone beds, so it remains unclear whether the low-angle cross lamination is foreset or backset.

We constructed geologic columns along traverses F1and F2 in Nagasaki (Fig. 5) where a 5 m-thick Sak

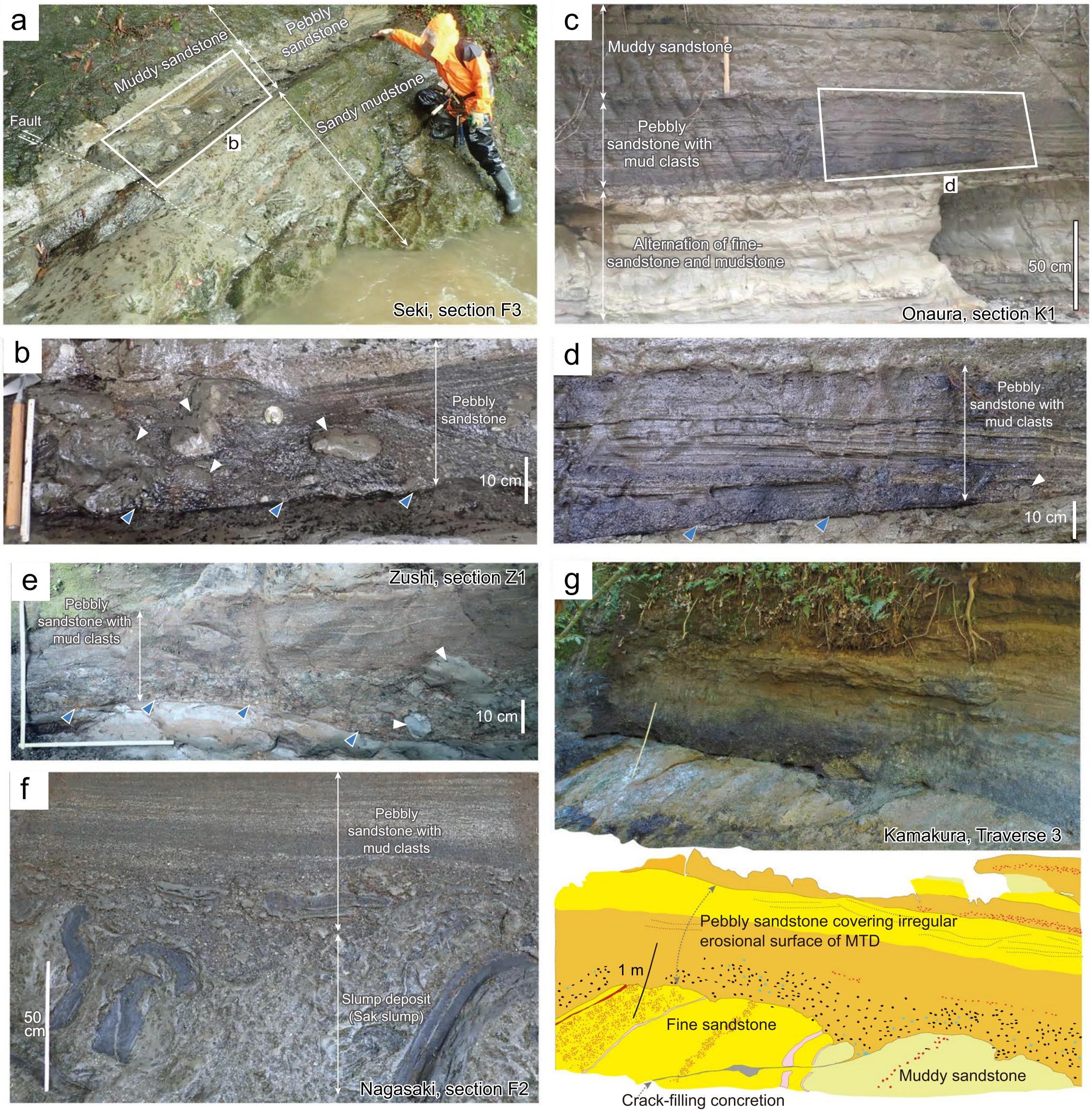

Fig. 7 Outcrops of **a**–**e** pebbly sandstone beds covering the major erosional surface and **f**, **g** coeval MTDs (mass-transport deposits) formed at around 3.2 Ma. **a**–**e** A poorly-sorted pebbly sandstone with mud clasts on the major erosional surface exposed at section F3 in Seki **a**, **b** on the western Boso Peninsula, **c**, **d** at section K1 on the eastern Boso Peninsula, and **e** section Z1 on the Miura Peninsula. See Figs. 3, 5c, 6 for the localities. **f**, **g** Mass-transport deposits exposed **f** in Nagasaki on the western Boso Peninsula and **g** along traverse 3 on the Miura Peninsula. See Fig. 5 and Utsunomiya et al. (2017) for the localities. Blue arrows in **b**, **d** and **e** indicate the major erosional surface. White arrows in **d** and **e** indicate the mud clasts

slump deposit is intercalated between tephra beds An156-4 and An157. In these sections, tuffaceous sandy mudstones (13 m thick) are successively exposed, and they overlie the Sak slump that consists of folded blocks of alternating beds of sandstone and sandy mudstone (Fig. 5). Most of the tephra beds in the uppermost part of the Anno Formation are coarse-ash-dominated beds and lapilli-dominated beds. The 40 cm-thick scoria-rich lapilli bed An158 (Nakajima 2005) is intercalated 11 m above the top of the sandstone that covers the Sak slump (Fig. 5d). Although Nakajima (2005) in a broad sense named a set of tephra beds that included An158 as An158 for the purposes of stratigraphic correlation, here, in a stricter sense, we consider just the 40 cm-thick scoria-rich lapilli bed as An158. Two fine vitric ash beds are intercalated below and above An158; herein, the lower vitric tephra bed is An157.5, and the upper bed is An158.5 (Fig. 5d).

The Kiyosumi and the lower part of the Anno formations are successively exposed along a branch stream of the Koito River in Okugome, Kimitsu City, in the central part of the Boso Peninsula (Additional file 1: Fig. A1), and this is where the marker tephra beds Ky25 and Ky26 are intercalated (Nakajima et al. 1981; Natural History Museum and Institute, Chiba, 1994). Ky26 is intercalated 6 m above Ky25 in the sandstone-dominated alternating beds of sandstone and mudstone (Additional file 1: Fig. A1).

4.1.3 Eastern Boso peninsula

The Kiyosumi Formation and the overlying Kurotaki and Katsuura formations are exposed at Onaura in Katsuura City (Fig. 6). These formations are cut by NE–SW-trending normal faults. The Kiyosumi Formation dips gently to the northeast and is overlain by the Kurotaki Formation, with the subparallel erosional surface displayed at section K1 (Fig. 7c, d).

At locality K1, a 50-cm-thick pebbly sandstone overlies the turbidite deposits of the Kiyosumi Formation on a subparallel erosional surface (Fig. 6). Unlike the submarine canyon fills with terrestrial links in the Kazusa Group (Yamauchi et al. 1990; Ito and Saito 2006), the sand and gravel of the scar fill is characterized by mud clasts that consist mainly of volcanic rocks and scoria, similar to the pyroclastic material in the Anno Formation. Rather than being massive sand and gravel, the sedimentary rocks display undulating parallel or low-angle cross stratification and are poorly sorted (Figs. 6, 7c, d). Calcareous nannofossil biozones in the underlying Kiyosumi and overlying Kurotaki formations can be assigned to CN10-CN11 and CN12a, respectively (Fig. 6). Above this, the muddy sandstone correlated with the Kurotaki Formation shows an upward-fining succession into the Katsuura Formation, in which angular unconformities can be observed (Figs. 6, 8a, b, d). The surface of the unconformity between geologic columns K2 and K3 (Fig. 6) is covered by a thin sand layer with burrow structures (Fig. 8d). This upward-fining succession has been interpreted as a transgression from shallow water into the sedimentary facies of a distal submarine fan of the Kazusa Group (Ito 1992b). Despite these angular unconformities, the temporal gap is within the CN12b subzone (2.8–2.5 Ma), and this gap is much smaller than that represented by the erosional base of the pebbly sandstone bed. Tephra bed Onr was first reported from the Kurotaki Formation (Fig. 6). We could not identify other marker tephra beds, most likely because of the coarser facies.

Channel-fill conglomerate (Kawabe et al. 1980; Ito 1992b; Ito et al. 1992) cuts all the sedimentary sequences described above at section K4 (Fig. 6). The erosional base of this conglomerate shows a staircase-like geometry (Fig. 8c, e). Calcareous nannofossil assemblages in the mudstone immediately above the channel-fill conglomerate indicate the CN12d subzone (2.5–2.0 Ma) at section K4, which is considerably younger than the erosional surface at section K1.

4.2 Descriptions and remarks on the chemical compositions of the tephra beds

Here we describe ten tephra beds, and for eight of these we determined the refractive indices of the glass shards and their chemical compositions.

4.2.1 Nt

Tephra bed Nt consists of a 37 cm-thick crystal-vitric lower unit (medium-sand to coarse-sand size), a 33 cm-thick crystal-vitric middle unit (coarse-sand size), and a 57 cm-thick crystal-vitric upper unit (silt size). These units would correspond to the Nt-1, Nt-2, and Nt-3 units described by Urabe (1998). The tephra sample from 10 cm above the base of Nt is a coarse crystal-vitric ash characterized by orthopyroxene as the dominant heavy mineral with a little hornblende and clinopyroxene. We did not determine the refractive indices or chemical compositions of the glass shards in this tephra bed.

4.2.2 Ng

Tephra bed Ng is a 15 cm-thick vitric ash bed consisting of a white-colored 8 cm-thick lower unit (very-fine-sand- to silt-sized) and a light-gray-colored 7 cm-thick upper unit (silt size) (Fig. 9). The boundary between the upper unit and the overlying tuffaceous mudstone is gradual. The heavy minerals are dominantly orthopyroxene along with hornblende and a little clinopyroxene and biotite (Table 1). Glass shards of bubble-wall, small bubble, stripe, sponge, and fiber types were observed (Table 1), and the refractive indices of the glass shards (n) range from 1.502 to 1.505 with a mode at 1.503–1.504 and with 1.498 as an outlier (Table 1). The glass shards contain 3.41 wt.% K_2O and have relatively high (583 ppm) values of Ba (Table 2).

4.2.3 IkT16

Tephra bed IkT16 is a white-colored 10–12 cm-thick vitric ash bed with very-fine-sand- to silt-sized particles (Fig. 9). Glass shards of small-bubble, stripe, and sponge types dominate over the bubble-wall type. Heavy minerals are rare in this tephra bed. The refractive indices of the glass shards (n) range from 1.507 to 1.511 with a mode at 1.509–1.510 (Table 1). The glass shards have relatively low SiO_2 (76.95 wt.%) and K_2O (1.15 wt.%) contents compared with the other analyzed

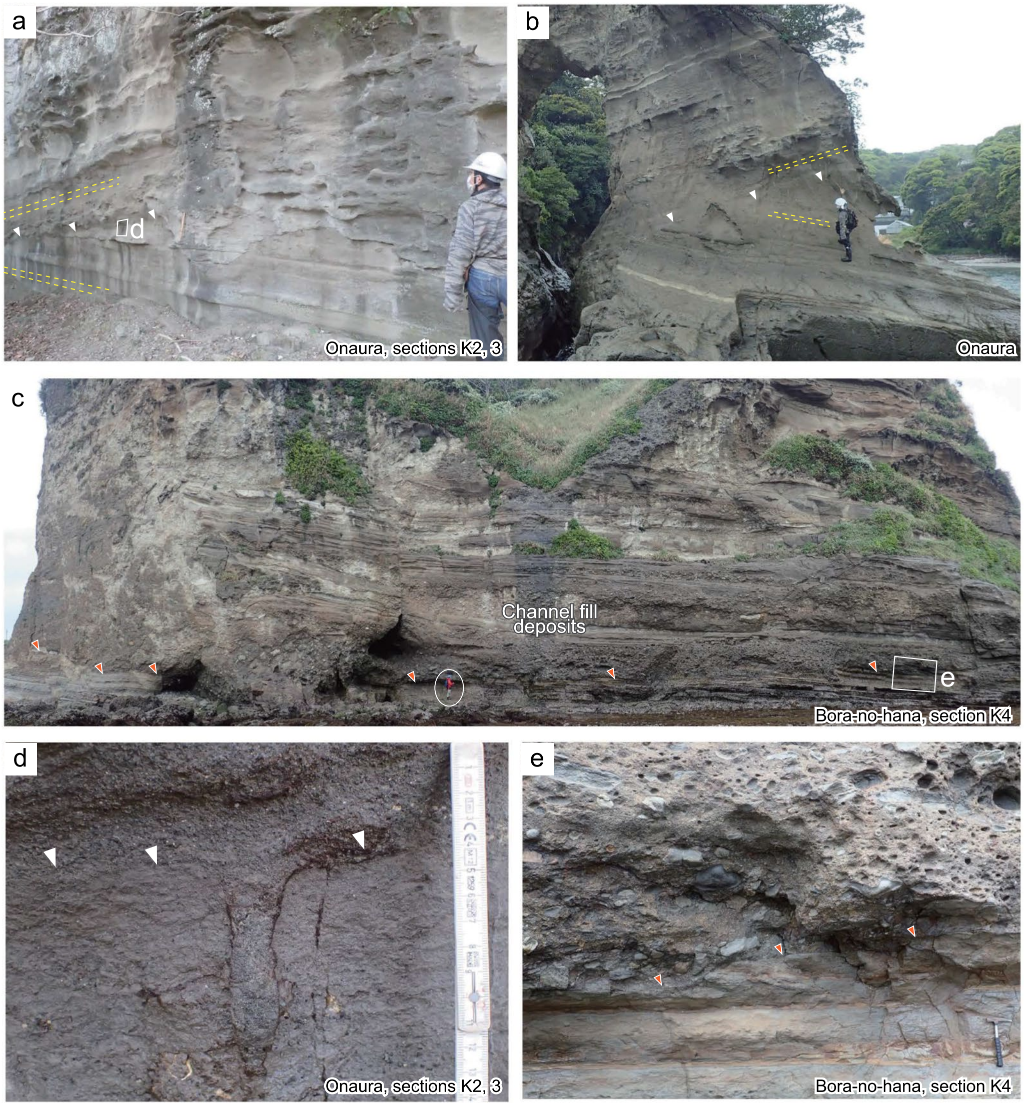

Fig. 8 Outcrops of the angular unconformity **a**, **b**, **d** and channel fill deposits **c**, **e** in the Kurotaki Formation, which are dated between 2.8–2.5 and 2.5–2.0 Ma, younger than the major erosional event. **a** Angular unconformity exposed in the quarry cliff at Loc. K3. **b** Angular unconformity exposed in the sea cliff. **c** Channel fill deposits of conglomerate of the Kurotaki Formation overlying the Kiyosumi Formation at Loc. K4. **d** Close-up photograph of **a**. The angular unconformity is covered by a thin, volcaniclastic-rich fine-grained sand bed, which is laterally obscured due to bioturbation. A burrow cutting the underlying strata can be observed. **e** Close-up photograph of basal conglomerate of the channel fill deposits. Yellow dashed lines in **a** and **b** indicate the bedding plane. The white arrows in **a**, **b**, and **d** indicate the angular unconformity. Red arrows in **c** and **e** indicate the erosional surface underlying the channel-fill deposits

tephra beds but relatively high FeO (2.51 wt.%), CaO (2.44 wt.%), and Al_2O_3 (12.59 wt.%) contents (Table 2).

4.2.4 IkT19

Tephra bed IkT19 is a white-colored 6–7 cm-thick vitric ash bed with a very-fine sand to silt grain size (Fig. 9). Coarse-sand- to granule-sized pumice grains are scattered immediately below this tephra bed. Glass shards of bubble-wall type dominate over the other types. Heavy minerals are rare in this tephra bed. The refractive indices of the glass shards (n) range from 1.500 to 1.506 with a mode at 1.503–1.504 (Table 1). The glass shards have relatively low SiO_2 (78.43 wt.%) and K_2O (1.47 wt.%) contents and slightly high contents of Y (44.7 ppm) (Table 2).

4.2.5 Ahn

Tephra bed Ahn is a white-colored 6 cm-thick vitric ash bed with a silt grain size (Fig. 9). A fine-grained sandstone bed is intercalated immediately below this tephra. Glass

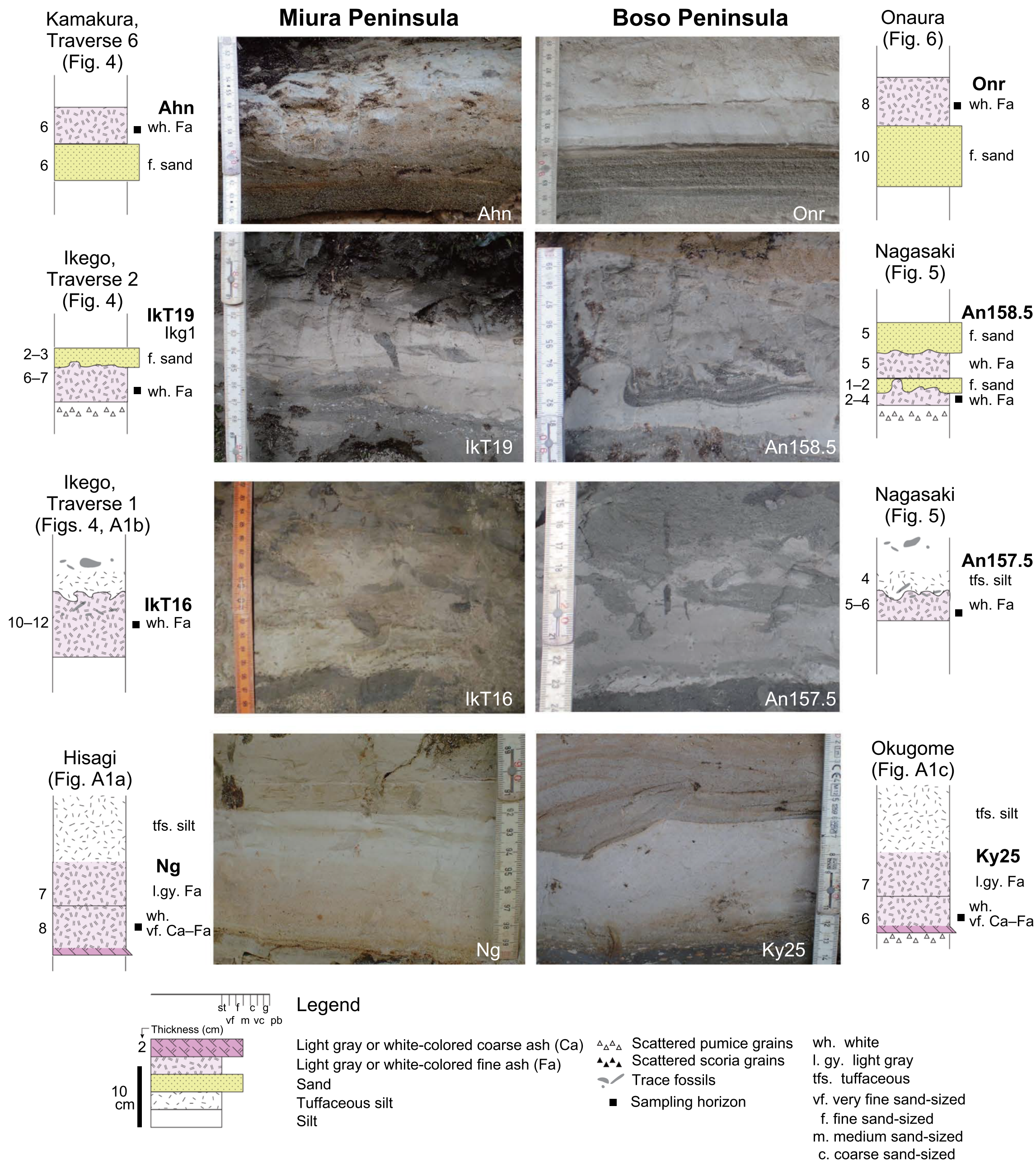

Fig. 9 Geologic columns showing lithologies and sampling horizons, and photographs of the correlated tephra beds

shards of bubble-wall and stripe types dominate over the other types. The heavy minerals are dominated by biotite, with a small amount of orthopyroxene (Table 1). The refractive indices of the glass shards (n) range from 1.498 to 1.500 (Table 1). The glass shards have relatively low contents of SiO_2 (77.31 wt.%), FeO (0.98 wt.%), and CaO (0.78 wt.%) and slightly high contents of K_2O (4.80 wt.%) (Table 2).

4.2.6 Ky26

Tephra bed Ky26 consists of a 22 cm-thick crystal-vitric lower unit (medium-sand to coarse-sand size), a 29 cm-thick crystal-vitric middle unit (coarse-sand size), and a 100 cm-thick crystal-vitric upper unit that shows convolute lamination (silt size). These units correspond to the Nt-1, Nt-2, and Nt-3 units described by Urabe (1998). The tephra sample obtained 10 cm

Table 1 List showing location, glass type and refractive index of the tephra layers

Tephra name	Locality	Latitude, longitude	Shape of glass shards*	Dominated heavy mineral	Refractive index of volcanic glass (n)
Ahn (AhG)	Juniso, Kamakura City	35°20′01.2"N 139°34′49.0"E	bw, str	bi > opx	1.498–1.500
Onr	Onaura, Katsuura City	35°08′27.4"N 140°17′24.5"E	bw, str	bi > opx, ho	1.497–1.499
IkT19 (Ikg1)	Ikego, Zushi City	35°18′37.4"N 139°36′30.3"E	bw > str, sb, fib, spg	-	1.500–1.506
An158.5	Nagasaki, Futtsu City	35°13′20.9"N 139°54′34.5"E	bw > str, sb, fib, spg	-	1.500–1.507
IkT16	Ikego, Zushi City	35°18′34.8″ N 139°36′35.6″ E	sb, spg, str > bw	-	1.507–1.511
An157.5	Nagasaki, Futtsu City	35°13′19.6"N 139°54′39.0"E	sb, spg, fib, str > bw	-	1.508–1.510, 1.513
Ng	Hisagi, Zushi City	35°18′27.2"N 139°34′07.0"E	bw, str, sb, spg, fib	opx > ho > > cpx, bi	1.498, 1.502–1.505
Ky25	Okugome, Kimitsu City	35°10′41.9"N 140°02′09.3"E	bw, str, sb, spg, fib	opx > ho, cpx > > bi	1.503–1.505

* Shapes of glass shards were classified on the basis of bubble shape and bubble size following Kishi and Miyawaki (1996): *bw* Bubble-wall type, *fib* Fiber type, *sb* Small-bubble type, *spg* Sponge type, *str* Stripe type. *ho* Hornblende, *opx* Orthopyroxene, *cpx* Clinopyroxene, *bi* Biotite

above the base of Nt consists of a coarse crystal-vitric ash with orthopyroxene as the dominant heavy mineral and minor hornblende and clinopyroxene. We did not determine the refractive indices and chemical compositions of the glass shards in this tephra bed.

4.2.7 Ky25

Tephra bed Ky25 is a 13 cm-thick vitric ash bed that consists of a white-colored 6 cm-thick lower unit (very-fine-sand- to silt-sized) and a light-gray-colored 7 cm-thick upper unit (silt size) (Fig. 9). The boundary between the upper unit and the overlying tuffaceous mudstone is gradual. The heavy minerals are dominated by orthopyroxene with some hornblende and clinopyroxene and a little biotite (Table 1). Glass shards of bubble-wall, small bubble, stripe, sponge, and fiber types were observed (Table 1). The refractive indices of the glass shards (n) range from 1.503 to 1.505 with a mode at 1.503–1.504 (Table 1). The glass shards contain 3.46 wt.% K_2O and have relatively high (542 ppm) contents of Ba (Table 2).

4.2.8 An157.5

Tephra bed An157.5 is a white-colored 5–6 cm-thick vitric ash bed of very-fine-sand- to silt-sized volcanic ash (Fig. 9). Glass shards of small-bubble, stripe, and sponge types dominate over the bubble-wall type. Heavy minerals are rare in this tephra bed. The refractive indices of the glass shards (n) range from 1.508 to 1.510, with a mode at 1.508–1.509 and with 1.513 as an outlier (Table 1). The glass shards have lower contents of SiO_2 (76.86 wt.%) and K_2O (1.15 wt.%) than the other analyzed tephra beds (Table 2) but higher contents of FeO (2.59 wt.%), CaO (2.47 wt.%), Al_2O_3 (12.56 wt.%), and Sr (136.2 ppm).

4.2.9 An158.5

Tephra bed An158.5 is a white-colored 2–4 cm-thick vitric ash bed of very-fine-sand- to silt-sized volcanic ash, and it is overlain by a 1–2 cm-thick fine sandstone bed and a 5 cm-thick white-colored fine ash bed in ascending order (Fig. 9). Coarse-sand- to granule-sized pumice grains are scattered immediately below this tephra bed. Glass shards of bubble-wall type dominate over the other types. Heavy minerals are rare. The refractive indices of the glass shards (n) range from 1.500 to 1.507 with a mode at 1.503–1.504 (Table 1). The glass shards have relatively low contents of SiO_2 (78.51 wt.%) and K_2O (1.53 wt.%) and slightly high contents of Y (47.3 ppm) (Table 2).

4.2.10 Onr

Tephra bed Onr is a white-colored 10 cm-thick vitric ash bed with a silt grain size (Fig. 9). A fine-grained sandstone bed is intercalated immediately below this tephra bed. Glass shards of bubble-wall and stripe types are dominant. The heavy minerals are dominantly biotite, along with a little orthopyroxene and hornblende (Table 1). The refractive indices of the glass shards (n) range from 1.497 to 1.499 (Table 1). The glass shards have relatively low contents of SiO_2 (77.34 wt.%), FeO (0.95 wt.%), and CaO (0.80 wt.%) but relatively high contents of K_2O (4.76 wt.%) (Table 2).

5 Discussion

5.1 Tephra correlation

Based on previous calcareous nannofossil biostratigraphic and magnetostratigraphic studies, the upper part of the Ikego Formation above the Jimmuji Member on the Miura Peninsula may be the time-equivalent of the uppermost part of the Anno Formation on the Boso Peninsula. In addition, the uppermost part of the Zushi Formation on the Miura Peninsula can be correlated with the uppermost part of the Kiyosumi Formation. The thicknesses, lithologic features, and compositions of minerals in Nt, Ng, IkT16, IkT19, and Ahn on the Miura Peninsula

Table 2 Major and trace element compositions of the volcanic glass shards

Tephra name		Major element composition (wt.%)								
		SiO_2	TiO_2	Al_2O_3	FeO*	MnO	MgO	CaO	Na_2O	K_2O
Ahn (AhG)	Ave	77.31	0.06	12.63	0.98	0.08	0.06	0.78	3.29	4.80
Urago Fm	SD	0.17	0.04	0.09	0.07	0.06	0.03	0.05	0.08	0.14
Onr	Ave	77.34	0.08	12.70	0.95	0.07	0.04	0.80	3.26	4.76
Kurotaki Fm	SD	0.14	0.04	0.08	0.09	0.06	0.02	0.05	0.11	0.10
IkT19 (Ikg1)	Ave	78.43	0.25	12.15	1.55	0.09	0.28	1.98	3.79	1.47
Ikego Fm	SD	0.41	0.05	0.15	0.16	0.06	0.03	0.18	0.08	0.10
An158.5	Ave	78.51	0.25	12.10	1.54	0.09	0.25	1.89	3.84	1.53
Anno Fm	SD	0.26	0.06	0.15	0.10	0.07	0.03	0.10	0.07	0.08
IkT16	Ave	76.95	0.19	12.59	2.51	0.10	0.16	2.44	3.92	1.15
Ikego Fm	SD	0.19	0.07	0.08	0.14	0.07	0.05	0.08	0.07	0.06
An157.5	Ave	76.86	0.17	12.56	2.59	0.14	0.16	2.47	3.89	1.15
Anno Fm	SD	0.20	0.08	0.07	0.08	0.08	0.03	0.06	0.09	0.05
Ng	Ave	77.82	0.31	12.03	1.36	0.10	0.24	1.47	3.26	3.41
Zushi Fm	SD	0.23	0.06	0.09	0.07	0.07	0.06	0.05	0.20	0.30
Ky25	Ave	77.94	0.27	12.01	1.32	0.10	0.23	1.45	3.21	3.46
Kiyosumi Fm	SD	0.16	0.07	0.10	0.11	0.06	0.04	0.08	0.16	0.21
		Trace element composition (ppm)								
		Ba	**La**	**Sc**	**Sr**	**V**	**Y**		**Ba/La**	**La/Y**
Ahn (AhG)	Ave	658.19	26.09	6.29	66.53	0.83	19.64		25.2	1.3
Urago Fm	SD	29.60	1.77	0.88	5.31	0.07	1.67			
Onr	Ave	638.93	26.27	4.95	76.63	0.34	21.67		24.3	1.2
Kurotaki Fm	SD	29.31	1.98	0.63	5.90	0.14	1.34			
IkT19	Ave	480.9	16.0	12.1	118.1	4.3	44.7		30.0	0.4
Ikego Fm	SD	26.4	1.1	1.9	9.3	0.5	2.7			
An158.5	Ave	437.8	13.7	12.3	114.4	4.3	47.3		31.9	0.3
Anno Fm	SD	15.0	1.1	1.6	7.0	0.3	2.6			
IkT16	Ave	284.9	12.4	19.7	140.6	0.2	33.6		23.0	0.4
Ikego Fm	SD	17.1	0.6	1.5	11.8	0.1	2.0			
An157.5	Ave	287.6	12.6	19.6	136.2	0.1	34.1		22.8	0.4
Anno Fm	SD	14.8	0.9	1.6	8.3	0.1	2.0			
Ng	Ave	583.4	16.4	10.4	91.8	9.7	35.0		35.5	0.5
Zushi Fm	SD	19.4	1.3	1.9	7.9	0.8	2.2			
Ky25	Ave	542.8	14.9	9.9	86.6	8.0	32.3		36.4	0.5
Kiyosumi Fm	SD	16.6	1.0	1.0	6.3	0.8	1.8			

FeO*: total Fe calculated as FeO

and Ky26, Ky25, An157.5, An158.5, and Onr on the Boso Peninsula are in good agreement with each other, as are the shapes, refractive indices, and major-element compositions of their glass shards (Figs. 9, 10, Tables 1, 2). The minor-element compositions of these tephra beds are also similar (Table 2). The depositional ages of these tephra beds will be discussed below.

The mudstone immediately below Nt was assigned to the CN10c subzone of Okada and Bukry (1980), which is defined as the interval between the LAD (last appearance of datum) of *Ceratolithus acutus* (5.3 Ma) and the LAD of *Amaurolithus* spp. (4.5 Ma) (Kanie et al. 1991). Kameo et al. (2010) determined the LAD of *Amaurolithus* spp. (4.5 Ma) to be between the Ky29 and Ky31 tephra beds in the studied traverse along the branch stream of the Koito River in Okugome. They also demonstrated stratigraphic variations in the sizes of the coccoliths *Reticulofenestra* spp., and they assigned Ky25 and Ky26 to the intervals IIa of Kameo and Bralower (2000) and A1 of Takayama (1993). They interpreted Ky25 and Ky26 to be above the C3n.3n normal subchronozone (4.7–4.9 Ma), based on the chronostratigraphy established in ODP Hole 806B. Therefore, Ng and Ky25 can be correlated with each other on the basis of the

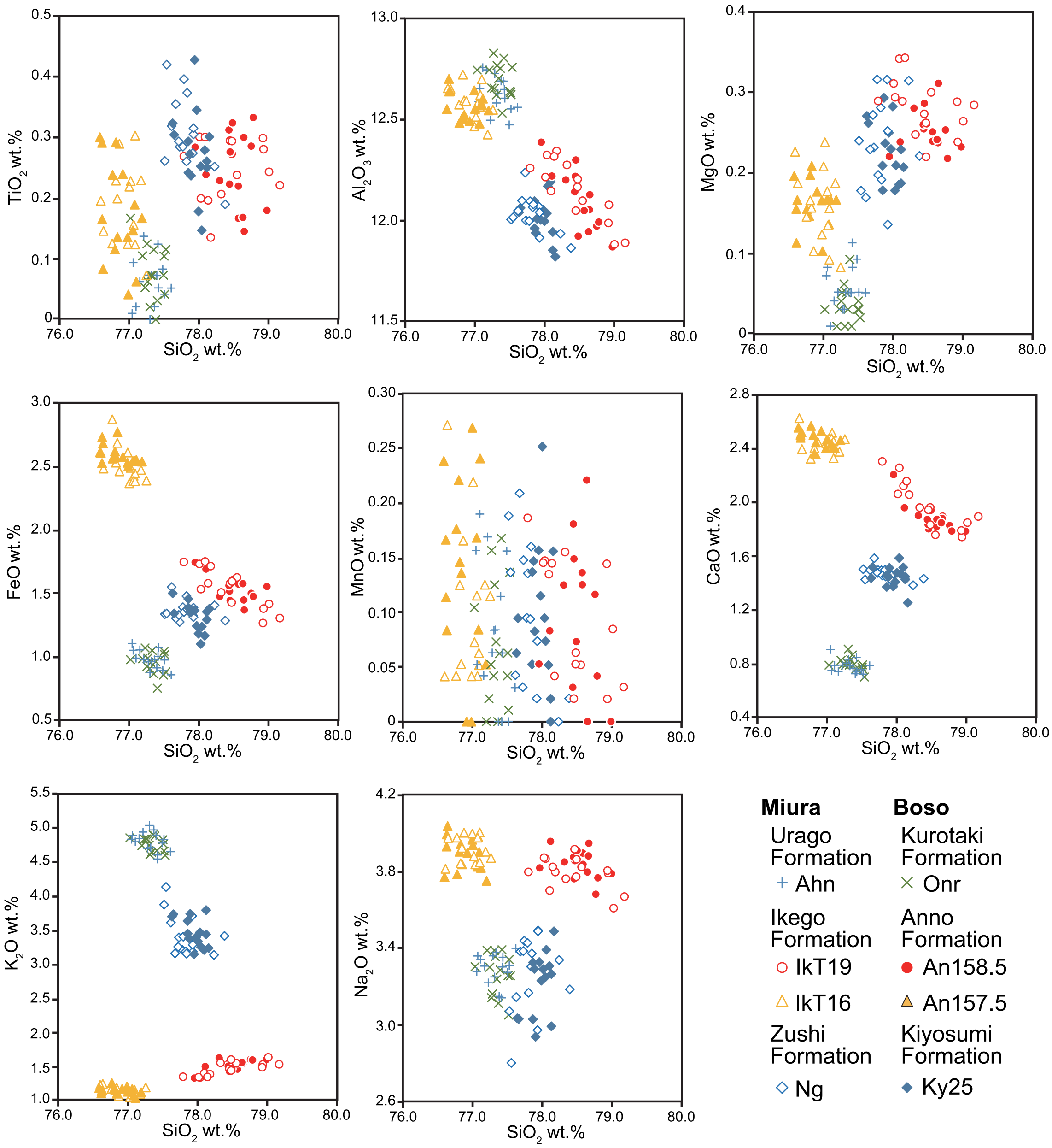

Fig. 10 Major element compositions of volcanic glass shards in the tephra beds

calcareous nannofossil biostratigraphy. This supports the correlation of Nt and Ky26, as suggested by previous researchers (Urabe et al. 1990; Suzuki et al. 1995).

IkT16 and IkT19 are located around the top (3.21 Ma) of the Mammoth subchronozone (C2An.2r) (Utsunomiya et al. 2017), and An158 is located above the top of the Mammoth subchronozone (Haneda and Okada 2019). Utsunomiya et al. (2017) showed that IkT19 is located in the normal subchronozone immediately above the Mammoth subchronozone (Additional file 1: Fig. A2). Normal polarity was detected immediately above IkT16, and reverse polarity was detected 2 m below IkT16 (Additional file 1: Fig. A2). Although An157.5 and An158.5 have not been reported from the Shikoma River (Haneda and Okada 2019), the top of the Mammoth subchronozone was estimated to be between 3.0 and 3.6 m below An158 (Haneda and Okada 2019). Therefore, IkT16 and IkT19 can be correlated with An157.5 and An158.5, respectively, which is consistent with the calcareous nannofossil biostratigraphy and magnetostratigraphy. The two tephra beds IkT16-An157.5 and IkT19-An158.5 are significant stratigraphic indicators for the top of the Mammoth subchronozone.

An158, a 40 cm-thick scoria-rich lapilli bed, can be traced laterally, whereas both the fine ash beds An157.5 and An158.5 (found in Nagasaki) are rare in Seki (Fig. 5d). The absence of fine ash beds is a probable result of strong bottom currents, which are considered to have been dominant when the coarser facies was deposited (Utsunomiya et al. 2015, 2017), and this can explain the absence of An157.5 and An158.5 in other areas.

Ahn is within the CN12b or CN12c subzones (Fig. 4), whereas Onr is within the CN12b subzone (Fig. 6). Ahn has been correlated with the widespread tephra UN-MD2, which has been assigned an age of 2.6–2.7 Ma (Tamura and Yamazaki 2010). The depositional ages are therefore consistent for both these tephra beds.

5.2 Major erosion at around 3.2 Ma and the resultant deposits

We have shown that the stratigraphic horizon between Nt-Ky26 and IkT16-An157.5 on the western side of the Boso Peninsula becomes remarkably thinner on the Miura Peninsula. Moreover, we have not found the widespread tephra beds of the Anno Formation (An51, An53, An77, An85, An112, An129, and An130) on the Miura Peninsula (Fig. 11a). To explain this, we will discuss here whether sedimentation rates were significantly different in the rocks of the Miura and Boso peninsulas. The thickness of the strata between Hk and Nt is ~ 200 m, based on the stratigraphy of Suzuki et al. (1995) and Eto (1986b, a), and the thickness between Ky21 and Ky26 is ~ 180 m, based on Tokuhashi and Ishihara (2008). Assuming the ages of Hk-Ky21 and Nt-Ky26 are ca. 4.9 Ma (near the base of C3n.3n: Niitsuma 1976 and Takahashi 2008) and ca. 4.7 Ma (above the top of C3n.3n), respectively, the rates of sedimentation between the two tephra beds are estimated to be ~ 100 cm/ky on the Miura Peninsula and ~ 90 cm/ky on the Boso Peninsula. The rates of sedimentation in the Mammoth subchronozone of the Anno Formation range from 9 to 66 cm/kyr (Haneda and Okada 2019), whereas the rates for the interval between the Mammoth and Kaena subchronozones in the upper part of the Ikego Formation range from 29 to 36 cm/kyr (Utsunomiya et al. 2017). Therefore, the thicknesses and sedimentation rates of the correlated stratigraphic intervals on the Miura Peninsula and the western Boso Peninsula do not differ markedly.

As an alternative idea, we can consider whether the Jimmuji Member and the Sak slump, which are mass-transport deposits, show that submarine landslide(s) contributed to the stratigraphic discontinuity. The age interval of the missing horizons is at least 1.3 Myr, if the top of the Zushi Formation and base of the upper part of the Ikego Formation are assigned ages of 4.5 Ma (top of *Amaurolithus* spp.) and 3.2 Ma (top of Mammoth subchronozone), respectively (Fig. 11b). A linear extrapolation using the sedimentation rate of the upper part of the Ikego Fomation (29–36 cm/kyr) suggests that at least 370-m-thick strata was eroded owing to the submarine landslide(s) that resulted in the formation of the Jimmuji Member.

The top of the Jimmuji Member and the top of the Sak slump are located 11 and 10 m below the IkT16-An157.5 tephra bed, respectively (Fig. 5). A similar stratigraphic level at the top of these deposits as well as residual blocks suggest that submarine landslide events resulted in the formation of both the Jimmuji Member and the Sak slump at the same time around 3.2 Ma.

In the eastern Boso Peninsula, a conglomerate in the K4 outcrop was considered by Ito et al. (1992) to have filled a channel that cut the Anno Formation during a sea-level lowstand during the early stage of formation of the Kurotaki unconformity. Some previous researchers have emphasized the role of submarine landslides as an essential erosional process, based on observations of the outcrop near section K4 (Kawabe et al. 1980; Otsubo et al. 2011). However, our geologic survey and biostratigraphic studies indicate that the Anno Formation had already been eroded away before the channel cut the strata sometime between 2.5 and 2.0 Ma. Rather than the channel deposits at section K4, the base of the pebbly sandstone bed at section K1 actually marks most of the major erosion in this area (Fig. 6). We could not identify the marker tephra bed immediately above the major erosional surface at section K1, and this resulted in a lack of an accurate age constraint (the CN12a zone lies between 3.5 and 2.76 Ma) for the major erosional surface in this region. Despite the uncertainties in the ages, we interpret the base of the Kurotaki Formation in the eastern Boso region to have been deposited immediately after the 3.2 Ma event (Fig. 11), based on the lithologic similarities of the pebbly sandstones and the bedding patterns and the consistency in nannofossil ages.

The basal pebbly sandstone pervasively covers a major erosional surface (Fig. 7) and consists of a poorly sorted pebbly sandstone that contains mud clasts and shows evidence of bed-load traction. These pebbly sandstone beds vary laterally into thick (up to 60 m) mass-transport deposits and into the overlying turbidite sandstones. Similar turbidite sandstones to those overlying the irregular upper surface of the MTD in this area have been reported from other MTDs (Yamamoto et al. 2007; Dykstra et al. 2011; Utsunomiya and Yamamoto 2019), and they become pebbly sandstone beds with sharp, flat erosional surfaces. The deposits resting on the basal

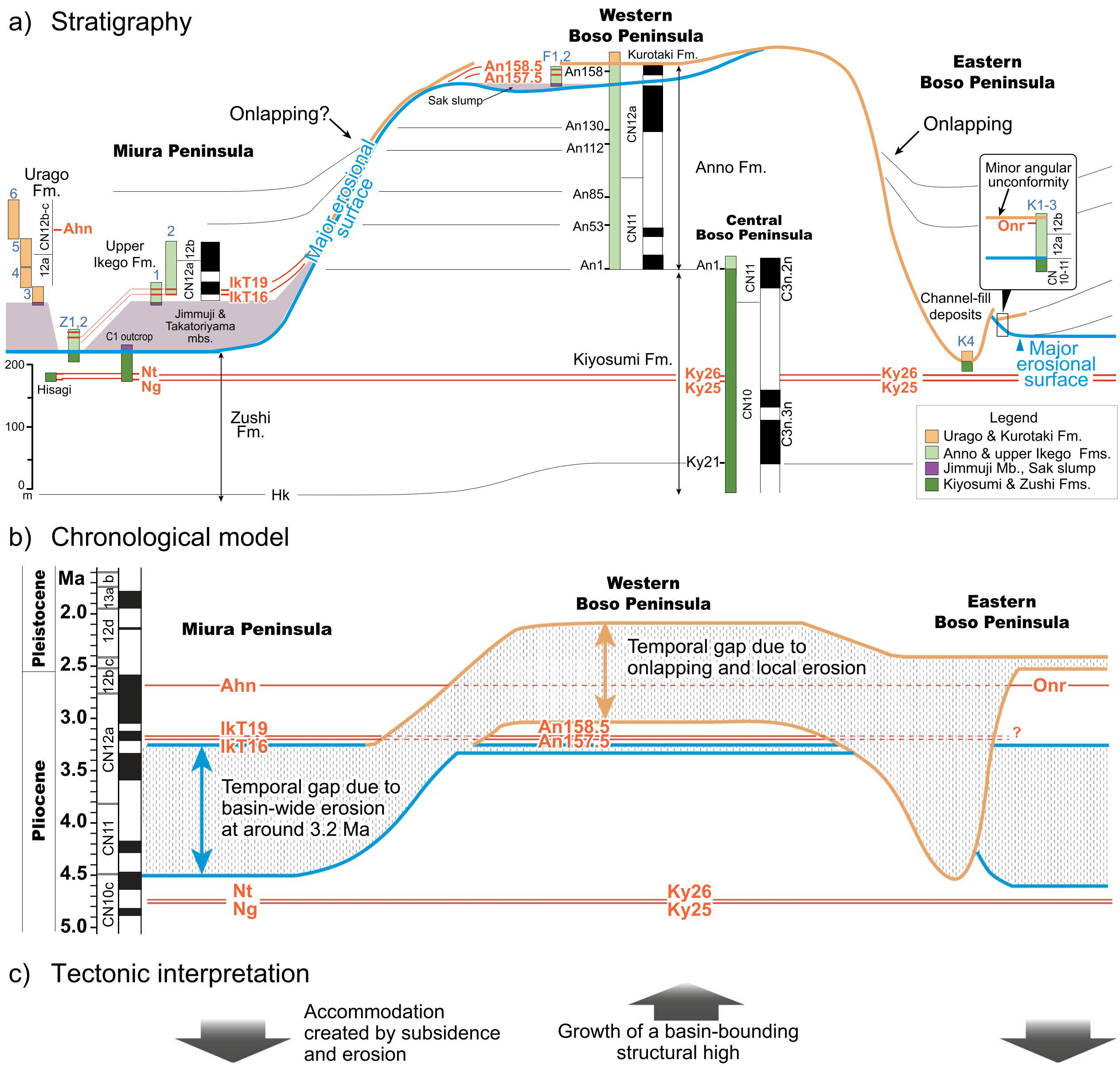

Fig. 11 Stratigraphic correlations and chronostratigraphic model with interpretation of regional relationships of subsidence and uplift that contributed to segmentation of the Miura–Boso forearc basin. **a** Stratigraphic correlations of the Miura, western Boso, and eastern Boso peninsulas. Stratigraphic divisions, calcareous nannofossil biostratigraphy, and magnetostratigraphy are based on our data sets and those of previous researchers (Urabe et al. 1990; Eto 1993; Eto et al. 1998; Kameo et al. 2010; Tamura and Yamazaki 2010; Kameo and Sekine 2013; Utsunomiya et al. 2017; Haneda and Okada 2019). **b** Stratigraphic model against a chronological axis. **c** Our interpretation of the regional relationships of subsidence and uplift that contributed to segmentation of the Miura–Boso forearc basin. The Kurotaki unconformity can be understood in terms of the major erosional event at around 3.2 Ma and several subsequent erosional events and overall onlapping deposition

erosional surfaces include a wide range of grain sizes, but they are dominated by granule- to pebble-sized pyroclastic fragments in medium–coarse-grained sandstones. Such coarse deposits are unusual in the lower part of the Kazusa Group, which is generally characterized by alternating beds of sheet-like turbidites and hemipelagic mudstones (Ito and Katsura 1992; Tokuhashi 1992; Utsunomiya 2019), suggesting a supply from lapilli beds in the collapsed section of the Anno Formation owing to a submarine landslide. Another candidate for a sedimentary source would be ocean-current-induced pyroclastic-rich sand-ridge deposits that formed on an upper slope, as seen in the Urago Formation (Utsunomiya et al. 2015), because it is possible to assume sand-ridge deposits were developed on the excavated upper slope. In either case, the pebbly sandstone would have been deposited rapidly, resulting in poor sorting.

5.3 Kurotaki unconformity and forearc basin segmentation

The stratigraphic context and tectonic significance of the Kurotaki unconformity between the Miura and Kazusa groups has long been debated following the work of Koike (1951). However, no previous researchers have discussed the differential erosional features described here, and we suggest that these features provide key information for explaining regional differences in the temporal gap. Here, we propose a new stratigraphic model that assumes the segmentation of the forearc basin by a residual topographic high into two distinct sub-basins (Fig. 11a). An important point in this model is that there is a time gap between ca. 3 and 2 Ma (Kameo and Sekine 2013) that compensates for the smaller amount of erosion at 3.2 Ma in the western Boso region (duration of 90 kyr, Haneda and Okada 2019) (Fig. 11b). This suggests the presence of a residual topographic high in the western Boso region, where sedimentation would have been punctuated, whereas the depressions created by erosional event(s) in the Miura and eastern Boso regions remained for the accommodation of subsequent deposits.

The Kazusa Group probably filled the field of subsidence in the eastern Boso region, as indicated by seismic surveys that showed strata more than 1000 m thick underlying the Katsuura Formation in the eastern offshore region of the Boso Peninsula (Okubo et al. 1990; Ozaki et al. 2019). In addition, there is no difference in the consolidation yield stresses of the Miura and Kazusa groups in the eastern Boso region, which suggests that this region was undergoing continuous subsidence while the western Boso region was being uplifted by tectonic movement (Kamiya et al. 2017, 2020). The thick lower part of the Kazusa Group offshore from the Boso Peninsula is presumed to thin and be draped on the major erosional surface toward section K1 on the eastern shore of the Boso Peninsula (Fig. 11a), and this situation is similar to the thin-bedded fine-grained turbidites that are draped over the slope (an aggradational onlap pattern; Smith and Joseph 2004). At section K1, we can therefore observe such layers that have been draped on the scarps of basin-wide submarine landslide(s), but they are generally too thin to be imaged using seismic data (Strasser et al. 2011). Similarly, syn-depositional subsidence would have occurred in the Miura region, because several hundred meters of sediment was deposited at paleobathymetries of 500–2000 m or 400–600 m (Eto et al. 1987; Utsunomiya and Majima 2012) after the major erosional event(s) that resulted in the formation of the Jimmuji Member. Our model therefore assumes uplift in the central to western Boso Peninsula but subsidence in the Miura Peninsula and eastern Boso Peninsula, thus inducing forearc basin segmentation (Fig. 11c).

Forearc basin segmentation is also observed in the basins that developed on the Pacific side of Japan, and these basins are divided by N–S trending topographic highs that were uplifted from the Pleistocene (Okamura 1990; Sugiyama 1992; Okamura and Blume 1993). The passage of undulations in the upper surface of the Philippine Sea Plate during its oblique subduction was considered to create alternating zones of uplift and subsidence in the forearc regions (Okamura and Shishikura 2020). The presence of middle Miocene igneous basement rocks around the Kii Peninsula would also enhance the segmentation of the forearc basin (Kimura et al. 2022). Oblique subduction is closely related to the change in direction of the Philippine Sea Plate from N to NW, but whether it occurred during the Pliocene (e.g., Seno and Maruyama 1984; Sugiyama 1992; Takahashi 2006, 2017) or Pleistocene (Nakamura et al. 1984) is subject to debate. The spatial switch of erosion and deposition in the forearc basins along the Pacific side of Japan would have occurred during this tectonic reconfiguration. Although tectonic reconstructions are beyond the scope of this paper because of the complicated and frequent changes in stress regime in this region (e.g., Angelier and Huchon 1987; Yamaji 2000; Otsubo et al. 2017; Utsunomiya and Otsubo 2022), additional data on the structure and orientation of folds and faults would be required, which together with our new stratigraphic framework, would help us reach a better understanding of the tectonic contribution to forearc basin segmentation.

6 Conclusions

We correlated the tephra beds that are intercalated in the forearc basin fill on the Miura and Boso peninsulas using stratigraphic levels, lithologic characteristics, and the chemical compositions of glass shards. The tephra correlations are consistent with the biostratigraphy and magnetostratigraphy established by our new work and that of previous researchers. These tephra beds are important chronological indicators, and they contribute to the construction of composite sections through the Pliocene in the forearc basin that can be used for studies of the regional paleoenvironment and basin evolution. We identified previously overlooked major erosional surfaces, which represent basin-scale mass-wasting event(s) that are associated with a disconformity in the upper Mammoth subchronozone (Mammoth event: 3.2 Ma). We present a new stratigraphic model that takes into account the geometry and lateral variation of the Kurotaki unconformity throughout the basin, and this is the first work on this unconformity since it was described 70 years ago by Koike (1951). The Mammoth event contributed to preservation of a continuous sedimentary record during the period 3.2 to 2.4 Ma on the eastern and western sides of the basin, whereas later local erosional event(s) occurred on the eastern side of the basin. The interaction between sedimentary systems and local relief owing to erosion and residual blocks in the mass transport deposits (MTDs), as well as bottom-current-induced bypassing of fine-grained sediments, had a major influence on the spatial–temporal variations in erosional thickness and sedimentation after the major erosional event at 3.2 Ma. This paper is the first to provide a detailed stratigraphic framework for the Miura–Boso forearc basin that is based on the concept of basin segmentation that resulted in differential erosion. We hope this work will further enhance our understanding of the evolution of forearc basins.

Supplementary Information

The online version contains supplementary material available at https://doi.org/10.1186/s40645-023-00558-y.

Additional file1 Fig. A1 Locations and route maps of the study sites. **Fig. A2** Geologic columns, stratigraphic distribution of calcareous nannofossils, and magnetic polarities in traverses 1 and 2 in the Ikego area, Miura Peninsula, after Utsunomiya et al.. **Fig. A3** Refractive indices of glass shards in the tephra beds.

Acknowledgements
The authors are grateful to Y. Haneda for providing information on stratigraphy and outcrops. S. Tokuhashi provided an unpublished geologic map showing the distribution of the Kiyosumi and Anno formations, which helped make the index map of the study area. We thank K. Mizuno for his help in determining the compositions of heavy minerals and glass shards. R. Majima is appreciated for his valuable suggestions and discussions on stratigraphy in the Miura Peninsula. We appreciate the help of H. Seto, K. Kanno, T. Izumi, K. Tanabe, and T. Konishi during the geological surveys around Zushi and Katsuura. Zushi City permitted and assisted our field survey in the Ikego Forest Natural Park, and we give particular thanks to Y. Sato for his assistance and support. South Kanto Defense Bureau confirmed the use of outcrop sketches. Editor J. B. H. Shyu is appreciated for careful handling and suggestions. The authors are grateful to G. F. Moore for his review and helpful comments. This study was supported by JSPS KAKENHI grant numbers JP17K18415 and JP20K14568.

Author contributions
MU proposed the topic and conceived and designed the study, and carried out geological field work and calcareous nannofossil biostratigraphy, developed the stratigraphic framework. IT carried out the tephra bed correlations. AN carried out geological field work, developed the stratigraphic framework with MU, and helped in the interpretations. TN collaborated with the corresponding author in the construction of the tephrostratigraphy. All authors read and approved the final manuscript.

Funding
This work was supported by JSPS KAKENHI grant numbers JP17K18415 and JP20K14568.

Availability of data and materials
The datasets supporting the conclusions of this article are included within the article and its additional files.
Declarations

Declarations

Competing interests
The authors declare that they have no competing interest.

Author details
[1]Research Institute of Geology and Geoinformation, Geological Survey of Japan, AIST, 1-1-1 Higashi, Tsukuba, Ibaraki 305-8567, Japan. [2]Chuo University, Higashinakano 742-1, Hachioji City, Tokyo 192-0393, Japan. [3]Hiratsuka City Museum, 12-41 Sengencho, Hiratsuka, Kanagawa 254-0041, Japan. [4]Tsukuba, Japan.

Received: 23 December 2022 Accepted: 28 April 2023
Published online: 17 May 2023

References

Akamine H, Iwai S, Koike K, Naruse Y, Ogose S, Omori M, Seki Y, Suzuki K, Watanabe K (1956) Geology of the miura peninsula. Earth Sci (chikyu Kagaku) 30:1–18 (in Japanese with English abstract)

Angelier J, Huchon P (1987) Tectonic record of convergence changes in a collision area: the Boso and Miura peninsulas, central Japan. Earth Plan Sci Lett 81:397–408

Asao K, Ito T (2011) Seismic reflection profile of the Kazusa-Shimosa group across the central Boso Peninsula, Japan. Abstract S3-O-4 presented at joint annual meeting of Japan Assoc Miner Sci and Geol Soc Japan 2011 (in Japanese)

Chiba Prefecture (2004) Report of Seismic geological survey in chiba prefecture. chiba prefecture, Japan (in Japanese)

Chiyonobu S, Sato T, Ishikawa K, Yamasaki M (2007) Uppermost Cenozoic calcareous nannofossil biostratigraphy of the hotspring wells located in the central part of Tokyo, Japan. J Geol Soc Japan 113:223–232 (in Japanese with English abstract)

Clift P, Vannucchi P (2004) Controls on tectonic accretion versus erosion in subduction zones: implications for the origin and recycling of the continental crust. Revi Geophys 42:RG2001

Dickinson WR (1995) Forearc basins. In: Busby C, Ingersoll RV (eds) Tectonics of sedimentary basins. Blackwell p, Oxford, pp 221–261

Dykstra M, Garyfalou K, Kertznus A, Kneller B, Milana JP, Molinaro M, Szuman M, Thompson P (2011) Mass-transport deposits: combining outcrop studies and seismic forward modeling to understand lithofacies distributions, deformation, and their seismic stratigraphic expression. In: Shipp RC, Weimer P, Posamentier HW (eds.) Mass transport deposits in deepwater settings p 293–310, SEPM (Society for sedimentary geology) Special Publication no 96, Tulsa

Eto T (1986a) Stratigraphy of the Hayama group in the Miura Peninsula, Japan. Sci Report Yokohama Nat Univ, Sec II 33:67–105 (in Japanese with English abstract)

Eto T (1986b) Stratigraphy of the Miura and Kazusa groups in the Miura Peninsula, Japan. Sci Report Yokohama Nat Univ, Sec II 33:107–132 (in Japanese with English abstract)

Eto T (1993) Geology of cutting outcrops in the Ikego US. facilities area in Zushi city, Kanagawa prefecture. Sci Report Yokohama Nat Univ, Sec II 40:31–51 (in Japanese with English abstract)

Eto T, Oda M, Hasegawa S, Honda N, Funayama M (1987) Geologic age and paleoenvironment based upon microfossils of the Cenozoic sequence in the middle and northern part of the Miura Peninsula. Sci Report Yokohama Nat Univ Sec II 34:41–57 (in Japanese with English abstract)

Eto T, Yazaki K, Urabe A, Isobe I (1998) Explanatory text of the geological map of Japan, Scale 1: 50 000, geology of the Yokosuka district (Tokyo—84). Geological survey of Japan, Tsukuba, 128 p (in Japanese with English abstract)

Fujioka M, Kameo K (2004) Correlation between the Obama formation of the Inubou group in the Choshi district and the Kiwada, Otadai and Umegase formations of the Kazusa group in the Boso Peninsula, central Japan, based on key tephra layers. J Geol Soc Japan 110:480–496 (in Japanese with English abstract)

Fujioka M, Kameo K, Kotake N (2003) Correlation based on key tephra layers between the Ofuna-Koshiba formations in the Yokohama district and the Kiwada formation in the Boso Peninsula, central Japan. J Geol Soc Japan 109:166–178 (in Japanese with English abstract)
Fuller CW, Willett SD, Brandon MT (2006) Formation of forearc basins and their influence on subduction zone earthquakes. Geology 34:65–68
Furusawa A (1995) Identification of tephra based on statistical analysis of refractive index and morphological classification of volcanic glass shards. J Geol Soc Japan 101:123–133 (in Japanese with English abstract)
Furusawa A (2017) Geochemical discrimination of individual glass shards from Towada-Ofudo and Towada-Hachinohe tephras using their trace element compositions determined by laser ablation ICP-MS. J Geol Soc Japan 123:765–776 (in Japanese with English abstract)
Haneda Y, Okada M (2019) Pliocene integrated chronostratigraphy from the Anno formation, Awa group, Boso Peninsula, central Japan, and its paleoceanographic implications. Prog Earth Planet Sci 6:6
Haneda Y, Okada M (2022) A record of the lower Mammoth geomagnetic polarity reversal from a marine succession in the Boso Peninsula, central Japan. Geophys J Int 228:461–476
Hatta A, Tokuhashi S (1984) On the foraminiferal assemblage in the hemipelagic mudstone of the Kiyosumi and anno formations, Boso Peninsula, Japan. News Osaka Micropaleontol (NOM) 12: 17–32 (inJapanese with English abstract)
Heiken G, Wohletz K (1985) Volcanic Ash. University of California Press, Berkeley
Hirayama J, Nakajima T (1977) Analytical study of turbidites, Otadai formation, Boso Peninsula, Japan. Sedimentology 24:747–779
Ida K, Mitsunashi T, Kageyama K (1956) On the new stratigraphic division of upper Cenozoic in Tokyo district. Bulletin Geol Surv Japan 7:435–436 (in Japanese with English abstract)
Inagaki S, Nishikawa T, Mitsuoka T, Yasuno M (2007) Garnet-bearing pumice bed, KGP, in the lower Kazusa group from the northeastern area of Kamakura City, Kanagawa prefecture, central Japan. Earth Sci (chikyu Kagaku) 61:143–148 (in Japanese with English abstract)
Ishihara Y, Tokuhashi S (2005) Depositional process of the Pliocene Anno formation, the uppermost part of the Awa group, Boso Peninsula, central Japan–a case study on a turbidite depositional system of a forearc-basin filling–. J Geol Soc Japan 111:269–285 (in Japanese with English abstract)
Ito M (1992a) High-frequencey depositional sequences of the upper part of the Kazusa group, a middle Pleistocene forearc basin fill in Boso Peninsula, Japan. Sed Geol 76:155–175
Ito M (1995) Volcanic ash layers facilitate high-resolution sequence stratigraphy at convergent plate margins: an example from the Plio-Pleistocene forearc basin fill in the Boso Peninsula, Japan. Sed Geol 95:187–206
Ito M, Katsura Y (1992) Inferred glacio-eustatic control for high-frequency depositional sequences of the Plio-Pleistocene Kazusa group, a forearc basin fill in Boso Peninsula, Japan. Sed Geol 80:67–75
Ito M, Kawabe T, O'hara S, (1992) Sequence stratigraphic analysis of the Pliocene Kurotaki formation, Boso Peninsula, Japan. J Sed Soc Japan 36:9–17
Ito M, Saito T (2006) Gravel waves in an ancient canyon: analogous features and formative processes of coarse-grained bedforms in a submarine-fan system, the lower Pleistocene of the Boso Peninsula, Japan. J Sed Res 76:1274–1283
Ito M, Kameo K, Satoguchi Y, Masuda F, Hiroki Y, Takano O, Nakajima T, Suzuki N (2016) Neogene–quaternary sedimentary successions. In: Moreno T, Wallis S, Kojima T, Gibbons W, eds., The geology of Japan, Geol Soc London, 309–337
Ito M (1992b) Chapter3: Sequence stratigraphy of the Kazusa group. In Makino, et al. (Eds) A Pliocene-Pleistocene fore-arc basin-fill in the Boso Peninsula, central Japan. 29th IGC Fieldtrip Guide A 10: 65–86.
Kameo K, Okada M (2016) Calcareous nannofossil biochronology from the upper Pliocene to lower Pleistocene in the southernmost Boso Peninsula, central part of the Pacific side of Japan. J Asian Earth Sci 129:142–151
Kameo K, Sekine T (2013) Calcareous nannnofossil biostratigraphy and geologic age of the Anno formation, the Awa group, in the Boso Peninsula, central Japan. J Geol Soc Japan 119:410–420 (in Japanese with English abstract)
Kameo K, Shindo R, Takayama T (2010) Calcareous nannofossil biostratigraphy and geologic age of the Kiyosumi Formation of the Awa group, Boso Peninsula, central Japan: age determination based on size variations of *Reticulofenestra* specimens. J Geol Soc Jpn 116:563–574 (in Japanese with English abstract)
Kameo K, Bralower T (2000) Neogene calcareous nannofossil biostratigraphy of sites 998, 999, and 1000, Caribbean Sea. In: R M Sigurdsson, H Acton, G D, and Draper G (Eds.), Proc ODP, Sci Results, 165:3–17. College Station, TX (Ocean Drilling Program)
Kamikuri S, Motoyama I, Nishi H, Iwai M (2009) Neogene radiolarian biostratigraphy and faunal evolution rates in the eastern equatorial Pacific ODP Sites 845 and 1241. Acta Palaeontol Pol 54:713–742
Kamiya N, Yamamoto Y, Wang Q, Kurimoto Y, Zhang F, Takemura T (2017) Major variations in vitrinite reflectance and consolidation characteristics within a post–middle miocene forearc basin, central Japan. Tectonophysics 710–711:69–80
Kamiya N, Yamamoto Y, Zhang F, Lin W (2020) Vitrinite reflectance and consolidation characteristics of the post-middle Miocene Forearc Basin in central and eastern Boso Peninsula, central Japan: Implications for basin subsidence. Isl Arc 29:e12344
Kanie Y, Okada H, Sasahara Y, Tanaka H (1991) Calcareous nannoplankton age and correlation of the Neogene Miura group between the Miura and Boso Peninsulas, southern-central Japan. J Geol Soc Japan 97:135–155 (in Japanese with English abstract)
Kasuya M (1987) Comparative study of Miocene fission-track chronology, and magnetobiochronology. Sci Rep Tohoku Univ 58:93–106
Kawabe T, Hamano S, Maeda S (1980) Some considerations on the forming of the late Pliocene-early Pleistocene Kurotaki formation, distributed in the Ubara district along the Pacific coast of the Boso Peninsula. J Geogr (chigaku Zasshi) 89:25–34
Kawabe T, Ohno K, Maeda S (1981) Some considerations on the stratigraphic relationship between the late Cenozoic Katsuura and Kurotaki formations in the Katsuura district, Boso Peninsula. J Geogr (chigaku Zasshi) 90:1–13
Kazaoka O, Suganuma Y, Okada M, Kameo K, Head MJ, Yoshida T, Sugaya M, Kameyama S, Ogitsu I, Nirei H, Aida N, Kumai H (2015) Stratigraphy of the Kazusa group, Boso Peninsula: an expanded and highly-resolved marine sedimentary record from the lower and middle Pleistocene of central Japan. Quat Int 383:116–135
Kimura G, Koge H, Tsuji T (2018) Punctuated growth of an accretionary prism and the onset of a seismogenic megathrust in the Nankai trough. Prog Earth Planet Sci 5:78
Kimura G, Nakamur, Y, Shiraishi K, Fujie G, Kodaira S, Tsuji T, Fukuchi R, Yamaguchi A (2022) Nankai forearc structural and seismogenic segmentation caused by a magmatic intrusion off the Kii Peninsula. Geochem Geophys Geosyst 23: e21022GC01
Kishi K, Miyawaki R (1996) Plio-Pleistocene fold development in the Kashiwazaki plain and vicinity, Niigata prefecture. J Geogr (chigaku Zasshi) 105:88–112 (in Japanese with English abstract)
Koike K (1951) On "the Kurotaki unconformity." J Geol Soc Japan 57:143–156 (in Japanese with English abstract)
Kurokawa K, Higuchi Y (2004) Tephrostratigraphy and correlations of some Pliocene tephra beds (4–2 Ma) in the Niigata region, especially on the distribution of the tsp tephra bed, and widearea correlations to the YT tephra beds in the Himi group and the Boso Peninsula, central Japan. Mem Fac Educ Hum Sci Nat Sci Niigata Univ 7: 13–78 (in Japanese with English abstract)
McKenzie DP, Morgan WJ (1969) Evolution of triple junctions. Nature 224:125–133
Mitsunashi T (1973) Geologic development of south Kanto and Niigata sedimentary basins from Miocene to Pleistocene. Earth Sci (chikyu Kagaku) 27:48–65 (in Japanese with English abstract)
Mitsunashi T, Yamauchi S (1988) Tectonic evolution of the sedimentary basin of the Kazusa group, Kanto district. Japan Mem Geol Soc Japan 30:67–75 (in Japanese with English abstract)
Mitsunashi T, Yasukuni N, Shinada Y (1959) Stratigraphical section of the Kazusa group along the shores of the rivers Yoro and Obitsu. Bulletin Geol Surv Japan 10:83–98 (in Japanese with English abstract)
Mitsunashi T, Kikuchi T (1982) Explanatory text of the geological map of Japan, Scale 1: 50 000, Yokohama district (Tokyo–74). Geol Surv Japan, Tsukuba, 105

Mitsunashi T, Yazaki K, Kageyama K, Shimada T, Ono E, Yasukuni N, Kamata S (1961) Geological maps of the oil and gas field of Japan no 4, Futtsu-Otaki, scale 1: 50 000, 1 sheet. Geol Surv Japan
Mizuno K, Naya Y (2011) Correlation of drilling cores in the central Kanto Plain, based on correlation of widespread tephras and recognition of marine horizons. Annual report of investigation on geology and active faults in the coastal zone of Japan (FY2011). GSJ Interim Report 56:121–132 (in Japanese with English abstract)
Moore GF, Boston BB, Strasser M, Underwood MB, Ratliff RA (2015) Evolution of tectono-sedimentary systems in the Kumano Basin, Nankai trough forearc. Mar Petrol Geol 67:604–616
Nagahashi Y, Satoguchi Y, Yoshikawa S (2000) Correlation and stratigraphic eruption age of the pyroclastic flow deposits and wide spread volcanic ashes intercalated in the Pliocene-Pleistocene strata central Japan. J Geol Soc Japan 106:51–69 (in Japanese with English abstract)
Nakamura K, Shimazaki K, Yonekura N (1984) Subduction bending and education; present and Quaternary tectonics of the northern border of the Philippine Sea Plate. Bulletin de la Société Géologique de France S7-XXVI(2):221–243. https://doi.org/10.2113/gssgfbull.S7-XXVI.2.221
Nakajima T, Watanabe M (2005) Geology of Futtsu district. Quadrangle series, 1: 50 000, Futtsu, Geol Sur Japan AIST, 102
Nakajima T, Makimoto H, Hirayama J, Tokuhashi S (1981) Geology of the Kamogawa district, quadrangle series, 1: 50,000. Geol Surv Japan AIST 48
Nakajima T (2005) Chapter 3, Awa group. Geology of the Futtsu district, quadrangle series, 1: 50,000. Geol Sur Japan AIST 13–39 (in Japanese with English abstract)
Natural History Museum and Institute, Chiba (1994) Geoscience data: catalog of key beds in the middle part of the Miura group II, the edition of 1993. Natural history museum and institute, Chiba, Chiba (in Japanese, title translated)
Natural History Museum and Institute, Chiba (ed) (1995) Geoscience data: catalog of key beds in the upper part of the Miura Group I, the edition of 1994. Natural history museum and institute, Chiba, Chiba (in Japanese, title translated)
Natural History Museum and Institute, Chiba (1996) Geoscience data: catalog of key beds in the upper part of the Miura group II, the edition of 1995. Natural history museum and institute, Chiba, Chiba (in Japanese, title translated)
Naya T, Hiramatsu C, Furusawa A, Yanagisawa Y, Yamaguchi K (2013) Chronostratigraphy of 1505 m long hot spring well drilled in the central Kanto plain, central Japan. J Geol Soc Japan 119:375–395 (in Japanese with English abstract)
Niitsuma N (1976) Magnetic stratigraphy in the Boso Peninsula. J Geol Soc Japan 82:163–181 (in Japanese with English abstract)
Noda A (2016) Forearc basins: types, geometries, and relationships to subduction zone dynamics. Geol Soc Am Bull 128:879–895
Oda M, Chiyonobu S, Torii M, Otomo T, Morimoto J, Satou Y, Ishikawa H, Ashikawa M, Tomonaga O (2011) Integrated magnetobiochronology of the Pliocene−Pleistocene Miyazaki succession, southern Kyushu, southwest Japan: implications for an early Pleistocene hiatus and defining the base of the Gelasian (P/P boundary type section) in Japan. J Asian Earth Sci 40:84–97
Ogawa Y, Seno T, Akiyoshi H, Tokuyama H, Fujioka K, Taniguchi H (1989) Structure and development of the Sagami trough and the Boso triple junction. Tectonophysics 160:135–150
Ogg JG (2020) Geomagnetic polarity time scale. In: Gradstein FM, Ogg JG, Schmitz M, Ogg G (eds) The geologic time scale 2020, vol 1. Elsevier, Amsterdam, pp 159–192
Okada H, Bukry D (1980) Supplementary modification and introduction of code numbers to the low-latitude coccolith biostratigraphic zonation (Bukry, 1973, 1975). Mar Micropaleontology 5:321–325
Okada M, Niitsuma N (1989) Detailed paleomagnetic records during the Brunhes—Matuyama geomagnetic reversal, and a direct determination of depth lag for magnetization in marine sediments. Phys Earth Planet Interiors 56:133–150
Okada H (1993) Results of analysis of the calcareous nannofossils from the specimens related to the Investigation of *Calyptogena* Fossils. In: Yokohama defence facilities administration Bureau (Ed.), Investigation of *Calyptogena* Fossils at Ikego, Final report p313–324 (in Japanese, title translated)
Okamura Y (1990) Geologic structure of the upper continental slope off Shikoku and quaternary tectonic movement of the outer zone of southwest Japan. J Geol Soc Japan 96(3):223–237 (in Japanese with English abstract)
Okamura Y, Blume P (1993) Seismic stratigraphy of quaternary stacked progradational sequences in the southwest Japan forearc: an example of fourth order sequences in an active margin. Spec Publ Int Assoc Sediment 18:213–232
Okamura Y, Shishikura M (2020) New hypothesis to explain quaternary forearc deformation and the variety of plate boundary earthquakes along the Suruga-Nankai trough by oblique subduction of undulations on the Philippine sea plate. Earth, Planets Space 72:55
Okubo S, Tono S, Tonoko N (1990) Development process of the sedimentary basin at offshore Boso Peninsula in the south Kanto district, central Japan. Mem Geol Soc Japan 34:21–30 (in Japanese with English abstract)
Otsubo M, Utsunomiya M, Miyakawa A (2017) Reactivation of map-scale faults in response to changes in crustal stress: examples from Boso Peninsula, Japan. Quat Int 456:117–124
Otsubo M, Yamaguchi N, Nomura S, Kimura N, Naruse H (2011) Basal slip plane of the Kurotaki unconformity in the Boranohana area along the Pacific coast of the Boso peninsula, central Japan. Isl Arc 20:305–307
Ozaki M, Furuyama S, Sato T, Arai K (2019) 1: 200 000 Marine and land geological map of the eastern coastal zone of the Boso Peninsula and its explanation, especially with Quaternary crustal deformation. S-6. Seamless Geoinformation of coastal zone "eastern coastal zone of Boso Peninsula". Geol Surv Japan, AIST (in Japanese with English abstract)
Pickering KT, Souter C, Oba T, Taira A, Schaaf M, Platzman E (1999) Glacio-eustatic control on deep-marine clastic forearc sedimentation, Pliocene−mid-Pleistocene (c. 1180–600 ka) Kazusa group. SE Japan J Geol Soc 156:125–136
Raffi I, Backman J, Fornaciari E, Pälike H, Rio D, Lourens L, Hilgen F (2006) A review of calcareous nannofossil astrobiochronology encompassing the past 25 million years. Quat Sci Rev 25:3113–3137
Raffi I, Wade BS, Pälike H, Beu AG, Cooper R, Crundwell MP, Krijgsman W, Moore T, Raine I, Sardella R, Vernyhorova YV (2020) The neogene period. In: geologic time scale 2020, p 1141–1215, Elsevier
Saito T, Ito M (2002) Deposition of sheet-like turbidite packets and migration of channel-overbank systems on a sandy submarine fan: an example from the late Miocene-early Pliocene forearc basin, Boso Peninsula, Japan. Sed Geol 149:265–277
Sakai T (1990) Upper cenozoic in the Choshi district, Chiba prefecture, Japan. Litho, magneto- and radiolarian biostratigraphy. Bull Fac General Edu Utsunomiya Univ 23:1–34
Sato T, Takayama T (1988) Calcareous nannofossil zones of the quaternary. Mem Geol Soc Japan 30:205–217 (in Japanese with English abstract)
Satoguchi Y (1995) Tephrostratigraphy in the lower to middle Kazusa group in the Boso Peninsula, Japan. J Geol Soc Japan 101:767–782 (in Japanese with English abstract)
Satoguchi Y, Higuchi Y, Kurokawa K (2005) Correlation of the Ohta tephra bed in the Tokai group with a tephra bed in the Miura group, central Japan. J Geol Soc Jpn 111:74–86 (in Japanese with English abstract)
Satoguchi Y, Nagahashi Y (2012) Tephrostratigraphy of the Pliocene to middle Pleistocene series in Honshu and Kyushu Islands, Japan. Isl Arc 21:149–169
Seno T, Maruyama S (1984) Paleogeographic recontraction and origin of the Philippine sea. Tectonophysics 102(1):53–84
Smith R, Joseph P (2004) Onlap stratal architectures in the Grès d'Annot: geometric models and controlling factors. Geol Soc London Sp Pub 221:389–399
Soh W, Pickering KT, Taira A, Tokuyama H (1991) Basin evolution in the arc−arc Izu Collision zone, Mio-Pliocene Miura group, central Japan. J Geol Soc 148:317–330
Strasser M, Moore GF, Kimura G, Kopf AJ, Underwood MB, Guo J, Screaton EJ (2011) Slumping and mass transport deposition in the Nankai fore arc: Evidence from IODP drilling and 3-D reflection seismic data. Geochem Geophys Geosyst 12(5):n/a-n/a. https://doi.org/10.1029/2010GC003431
Sugiyama Y (1992) Neotectonics of the forearc zone and the Setouchi Province in southwest Japan. Mem Geol Soc Japan 40:219–233 (in Japanese with English abstract)

Suzuki H, Horiuchi S (2002) Calcareous nannofossils analysis of the geological samples obtained from the deep observation boreholes in the Kanto plain. Report Res Product Nat Res Inst Earth Sci Disaster Prevent 225:1–71 (in Japanese with English abstract)

Suzuki T, Nakayama T (2007) A 2.0 Ma Widespread Tephra Associated with a Large-Scale Pyroclastic Flow from the Sengan Geothermal Area, Northeast Japan Arc. Bulletin Volcanol Soc Japan 52:23–38 (in Japanese with English abstract)

Suzuki S, Kanie Y (2012) Radiolarian biostratigraphy of the Pliocene Ikego formation, eastern Kanagawa prefecture. Res Rep Kanagawa Pref Mus Nat Hist 14:127–136 (in Japanese with English abstract)

Suzuki T, Murata M (2011) Stratigraphy and correlation of tephras in the lower Pleistocne Kiwada formation and its correlative beds, Kanto, central Japan. J Geol Soc Japan 117:379–397 (in Japanese with English abstract)

Suzuki Y, Kodama K, Mitsunashi T, Oka S, Urabe A, Endo T, Horiguchi M, Eto T, Kikuchi T, Yamauchi S, Nakajima T, Tokuhashi S, Nirei H, Hara Y, Nakayama T, Nasu N, Kagami H, Kimura M, Honza E (1995) Geology of the Tokyo bay and adjacent areas: miscellaneous map series 20, scale 1:100 000, 2 sheets. Geol Surv Japan Tsukuba 109 (in Japanese with English abstract)

Taira A, Eto T, Kanie Y (1993) Depositional environment of *Calyptogena*-bearing strata and seepage in deep sea floor. In: Yokohama defence facilities administration bureau (ed.), Investigation of *Calyptogena* fossils at Ikego, Final report, 65–96 (in Japanese title translated)

Takahashi M (2006) Tectonic development of the Japanese islands controlled by Philippine sea plate motion. J Geogr (chigaku Zasshi) 115:116–123 (in Japanese with English abstract)

Takahashi N, Mitsuoka T, Katoh A, Yokoyama K (2005) Correlation of the key tephra bed 'Kd38' occurring near the boundary between the Tertiary and quaternary in the southern part of the Kanto province, central Japan: correlation in the Kazusa group and the Chikura group, Boso Peninsula. J Geol Soc Japan 111:371–388

Takahashi M (2008) Southern Kanto. In: regional geology of Japan, part 5: Kanto district. Asakura Publishing, Tokyo 166–193 (in Japanese)

Takahashi M (2017) The cause of the east–west contraction of Northeast Japan. Bull Geol Surv Japan 68:155–161

Takano O, Itoh Y, Kusumoto S (2013) Variation in forearc basin configuration and basin-filling depositional systems as a function of trench slope break development and strike-slip movement: examples from the Cenozoic Ishikari–Sanriku-Oki and Tokai-Oki–Kumano-Nada forearc basins, Japan. In: Itoh, Y (ed.) Mechanism of sedimentary basin formation: multidisciplinary approach on active plate margins: Rijeka, Croatia, InTech, p 3–25

Takayama T (1993) Notes on neogene calcareous nannofossil biostratigraphy of the ontong java plateau and size variations of *Reticulofenestra* coccoliths. In: Berger W H, Kroenke L W, Mayer L A, et al., Proc ODP, Sci Res 130: 179–229, College station, TX (Ocean drilling program)

Tamura I, Mizuno K, Utsunomiya M, Nakajima T, Yamazaki H (2019) Widespread tephra of the Kazusa group distributed in the Boso Peninsula, Chiba prefecture, Japan: especially, tephrostratigraphy and tephra correlation of the lower part of the Kazusa Group. J Geol Soc Japan 125:23–39 (in Japanese with English abstract)

Tamura I, Takagi H, Yamazaki H (2010) The Tanzawa-garnet pumice: widely distributed 2.5 Ma tephra in the southern Kanto area. Japan J Geol Soc Japan 116:360–373 (in Japanese with English abstract)

Tamura I, Yamazaki H (2010) Significance of the remarkable unconformity in the Plio-Pleistocene of the Japanese islands. Quat Int 219:45–54

Tamura I, Yamazaki H, Mizuno K (2005) The Sakai volcanic ash and its correlatives: a 4.1 Ma (early Pliocene) widespread tephra in Japan. J Geol Soc Jpn 111:727–736 (in Japanese with English abstract)

Tamura I, Yamazaki H, Mizuno K (2008) Characteristics for the recognition of Pliocene and early Pleistocene marker tephras in central Japan. Quat Int 178:85–99

Tamura I, Yamazaki H, Mizuno K (2014) The age of the Inubou group in the Choshi district, Chiba prefecture, Japan, based on tephra correlation. Abstract HQR24–04 presented at Japan geoscience union meeting 2014

Tokuhashi S (1976a) Sedimentological study of the flysch-type alternation of Hk horizon in the Kiyosumi formation (part I): constitution of the alternation and form of individual sandstone bed. J Geol Soc Japan 82:729–738

Tokuhashi S (1976b) Sedimentological study of the flysch-type alternation of Hk horizon in the Kiyosumi formation (part II):depositional processes and circumstances of sandstone beds. J Geol Soc Japan 82:757–764

Tokuhashi S (1992) Paleocurrent of the turbidite sandstones in the upper Pliocene Katsuura formation of the lowermost Kazusa group, Boso Peninsula, central Japan. J Geol Soc Japan 98:943–952 (in Japanese with English abstract)

Tokuhashi S, Danhara T, Iwano H (2000) Fission track ages of eight tuffs in the upper part of the Awa group, Boso Peninsula, central Japan. J Geol Soc Jpn 106:560–573 (in Japanese with English abstract)

Tokuhashi S (1989) Two-stages of submarine-fan sedimentation in an ancient forearc basin, central Japan. In: Taira A, Masuda F (eds) Sedimentary facies in the active plate margin. Terrapub, pp 439–468

Tokuhashi S, Ishihara Y. (2008) Geological map in and around the forest Park, "Seiwa-Kenmin-no-Mori" in Chiba prefecture, Boso Peninsula, Central Japan. 1:15,000, Miscellaneous map series, Geol Surv Japan, AIST

Tréhu AM, Blakely RJ, Williams MC (2012) Subducted seamounts and recent earthquakes beneath the central Cascadia forearc. Geology 40:103–106

Ueki T, Hara H, Ozaki M (2013) Geology of the Hachioji district. Quadrangle series, 1: 50 000. Geol Surv Japan, AIST, p 137

Underwood MB, Moore GF (2012) Evolution of sedimentary environments in the subduction zone of southwest Japan: recent results from the NanTroSEIZE Kumano transect. In: Busby C, Azor, (eds) Tectonics of sedimentary basins: recent advances, 1st edn. Blackwell Publishing Ltd, USA

Urabe A (1992) Correlation of some pyroslastic key beds in the Mio-Pliocene Miura group, Miura and Boso Peninsulas, central Japan–reconstruction with additional data on heavy mineral composition and chemical composition–. J Geol Soc Japan 98:415–434 (in Japanese with English abstract)

Urabe A, Same M, Akiyama S, Tsubaki K, Yamauchi S, Mitsunashi T (1990) Geological structure of the tertiary formations in the western part of the middle Boso Peninsula and Uraga strait, Kanto district. Japan Mem Geol Soc Japan 34:31–44

Urabe A (1998) Chapter V. Key tuff beds in the Miura group. In: Eto T et al. 1998 Explanatory text of the geological map of Japan, Scale 1: 50 000, geology of the Yokosuka district (Tokyo–84). Geol Sur Japan, Tsukuba, 52–65 (in Japanese with English abstract)

Utsunomiya M (2018) Distribution, age, and origin of a submarine landslide deposit in the Pleistocene Kiwada formation, forearc basin fill on the Boso Peninsula, east-central Japan: constraints from tephro- and biostratigraphy. Isl Arc 27:e12254

Utsunomiya M, Kusu C, Majima R, Tanaka Y, Okada M (2017) Chronostratigraphy of the Pliocene-Pleistocene boundary in forearc basin fill on the Pacific side of central Japan: constraints on the spatial distribution of an unconformity resulting from a widespread tectonic event. Quat Int 456:125–137

Utsunomiya M, Majima R (2012) Paleobathymetries of the Plio-Pleistocene Urago and Nojima formations, Kazusa group, Miura Peninsula, central Japan: revision on the basis of molluscan fossils from new localities. Fossils (palaeontol Soc Japan) 91:5–14 (in Japanese with English abstract)

Utsunomiya M, Majima R, Taguchi K, Wada H (2015) An in situ Vesicomyid-dominated cold-seep assemblage from the lowermost Pleistocene Urago formation, Kazusa group, Forearc basin fill on the Northern Miura Peninsula, Pacific side of central Japan. Paleontol Res 19:1–20

Utsunomiya M, Mizuno K, Naya T, Omura K, Nagai M (2020) Correlation between a tephra bed from deep (2038 m) underground below Chiba city, and Kd48 in the lowermost Kiwada formation (lower Pleistocene) on the Boso Peninsula. J Geogr (chigaku Zasshi) 129:355–374 (in Japanese with English abstract)

Utsunomiya M, Mizuno K, Tamura I (2019) Stratigraphic positions and characteristics of tephra beds in the lower to middle Kiwada formation (lower pleistocene), Kazusa group. Bulletin Geol Surv Japan 70:373–441 (in Japanese with English abstract)

Utsunomiya M, Otsubo M (2022) Forearc tectonics and submarine landslides recorded in the lower part of the Kazusa group, eastern Boso Peninsula. J Geol Soc Japan 128:265–280 (in Japanese with English abstract)

Utsunomiya, M (2019) Chapter 3, Kazusa group. Geology of the Kazusa-Ohara district, Quadrangle series, 1: 50,000. Geol Surv Japan, AIST, 11–33 (in Japanese with English abstract)

Utsunomiya M, Ooi S (2019) Geology of the Kazusa-Ohara district. Quadrangle series, 1:50,000, geological survey of Japan, AIST, 127

Utsunomiya M, Yamamoto Y (2019) Spatial distribution of mass-transport deposits deduced from high-resolution stratigraphy: the Pleistocene forearc basin, central Japan. In: Ogata K et al (Eds), Submarine landslides: subaqueous mass transport deposits from outcrops to seismic profiles. Geophysical monograph series, American Geophysical Union
Utsunomiya M, Noda A, Otsubo M. (2018) Preferential formation of a slide-plane of translational submarine landslide deposits in the Pleistocene forearc basin fill exposed on central Japan. In: Lintern G et al. (Eds.) Subaqueous mass movements and their consequences: assessing Geohazards, environmental implications and economic significance of subaqueous landslides. Geol Soc Sp Papers 477
Wells RE, Blakely RJ, Sugiyama Y, Scholl DW, Dinterman PA (2003) Basin-centered asperities in great subduction zone earthquakes: a link between slip, subsidence, and subduction erosion? J Geophys Res 108(B10):2507
Yamaji A (2000) The multiple inverse method applied to mesoscale faults in mid-quaternary sediments near the triple trench junction off central Japan. J Struct Geol 22:429–440
Yamamoto Y, Ogawa Y, Uchino T, Muraoka S, Chiba T (2007) Large-scale chaotically mixed sedimentary body within the Late Pliocene to Pleistocene Chikura group. Central Japan 16:505–507
Yamauchi S, Mitsunashi T, Okubo S (1990) Growth pattern of the early Pleistocene Higashihigasa submarine channel, Boso Peninsula, central Japan. J Geol Soc Japan 96:523–536
Yanagisawa Y, Watanabe M, Takahashi M, Tanaka Y, Kimura K, Hayashi H (2006) 3. 2. 4 Annual report of special project for earthquake disaster mitigation in urban areas, regional characterization of the crust in metropolitan areas prediction of strong ground motion (FY2005): 296–329 (in Japanese)
Yokohama defense facilities administration Bureau (1993) Investigation of *Calyptogena* Fossils at Ikego, final report, 470 p. Yokohama defense facilities administration Bureau, Yokohama (in Japanese title translated)

Publisher's Note

Springer Nature remains neutral with regard to jurisdictional claims in published maps and institutional affiliations.